


REVIEW ARTICLE

Open Access

Hybrid materials of 1D and 2D carbon allotropes and synthetic π -systems

Balaraman Vedhanarayanan^{1,2}, Vakayil K. Praveen^{1,2}, Gourab Das^{1,2} and Ayyappanpillai Ajayaghosh^{1,2} 

Abstract

Self-assembled synthetic hybrid materials are an important class of artificial materials with potential applications in various fields ranging from optoelectronics to medicine. The noncovalent interactions involved in the self-assembly process offer a facile way to create hybrid materials with unique and interesting properties. In this context, self-assembled hybrid materials based on carbon nanotubes (CNTs), graphene, and graphene derivatives such as graphene oxide (GO) and reduced graphene oxide (RGO) are of particular significance. These composites are solution processable, generally exhibit enhanced electrical, mechanical, and chemical properties, and find applications in the fields of light harvesting, energy storage, optoelectronics, sensors, etc. Herein, we present a brief summary of recent developments in the area of self-assembled functional hybrid materials comprising one-dimensional (1D) or two-dimensional (2D) carbon allotropes and synthetic π -systems such as aromatic molecules, gelators, and polymers.

Introduction

Scientific innovations and technological breakthroughs in various sectors require the design and development of novel materials. Many of the existing materials may not satisfy all the fundamental requirements of mankind. This understanding has encouraged researchers to develop hybrid materials that can exhibit properties superior to those of the individual components^{1,2}. As in other research fields, advancements in the area of synthetic hybrid materials have been inspired by the various natural creations observed in the biological world, such as bone (a combination of an organic component, collagen, and an inorganic component, phosphate mineral) and nacre (a mixture of an elastic biopolymer, chitin, and carbonate minerals)^{3,4}. Hybrid materials are usually formed by combining organic and inorganic substances as in the case of the above natural materials; however, in recent times, combinations of different

types of polymers, nanomaterials, and carbon allotropes such as CNTs and graphene have also been included in the broad area of composite hybrid materials.

While there are several strategies for preparing hybrid materials, molecular self-assembly using noncovalent interactions^{5–10} is considered a simple and efficient approach to the preparation of hybrid materials^{11–16}. The nanoscale and mesoscale ordering of the building blocks in these hybrid materials and the resultant morphological features determine their functional properties, which can be modified by exploiting the reversible and adaptive nature of noncovalent interactions^{17,18}. Different strategies, including complementary interactions, molecular recognition, and templating, have been employed to create self-assembled hybrid materials². Among these methods, strategies based on π – π interactions are found to be extremely suitable for making hybrid materials in combination with 1D and 2D carbon allotropes and thereby overcome a major drawback associated with solubility¹⁹. Thus, the development of hybrid materials from CNTs and graphene using noncovalent functionalization has emerged as an interesting strategy that retains the original electronic properties with minimum structural defects. In this review, we

Correspondence: Ayyappanpillai Ajayaghosh (ajayaghosh@niist.res.in)

¹Photosciences and Photonics Section, Chemical Sciences and Technology Division, CSIR-National Institute for Interdisciplinary Science and Technology (CSIR-NIIST), Thiruvananthapuram 695019, India

²Academy of Scientific and Innovative Research (AcSIR), CSIR-NIIST Campus, Thiruvananthapuram 695019, India

© The Author(s) 2018



Open Access This article is licensed under a Creative Commons Attribution 4.0 International License, which permits use, sharing, adaptation, distribution and reproduction in any medium or format, as long as you give appropriate credit to the original author(s) and the source, provide a link to the Creative Commons license, and indicate if changes were made. The images or other third party material in this article are included in the article's Creative Commons license, unless indicated otherwise in a credit line to the material. If material is not included in the article's Creative Commons license and your intended use is not permitted by statutory regulation or exceeds the permitted use, you will need to obtain permission directly from the copyright holder. To view a copy of this license, visit <http://creativecommons.org/licenses/by/4.0/>.

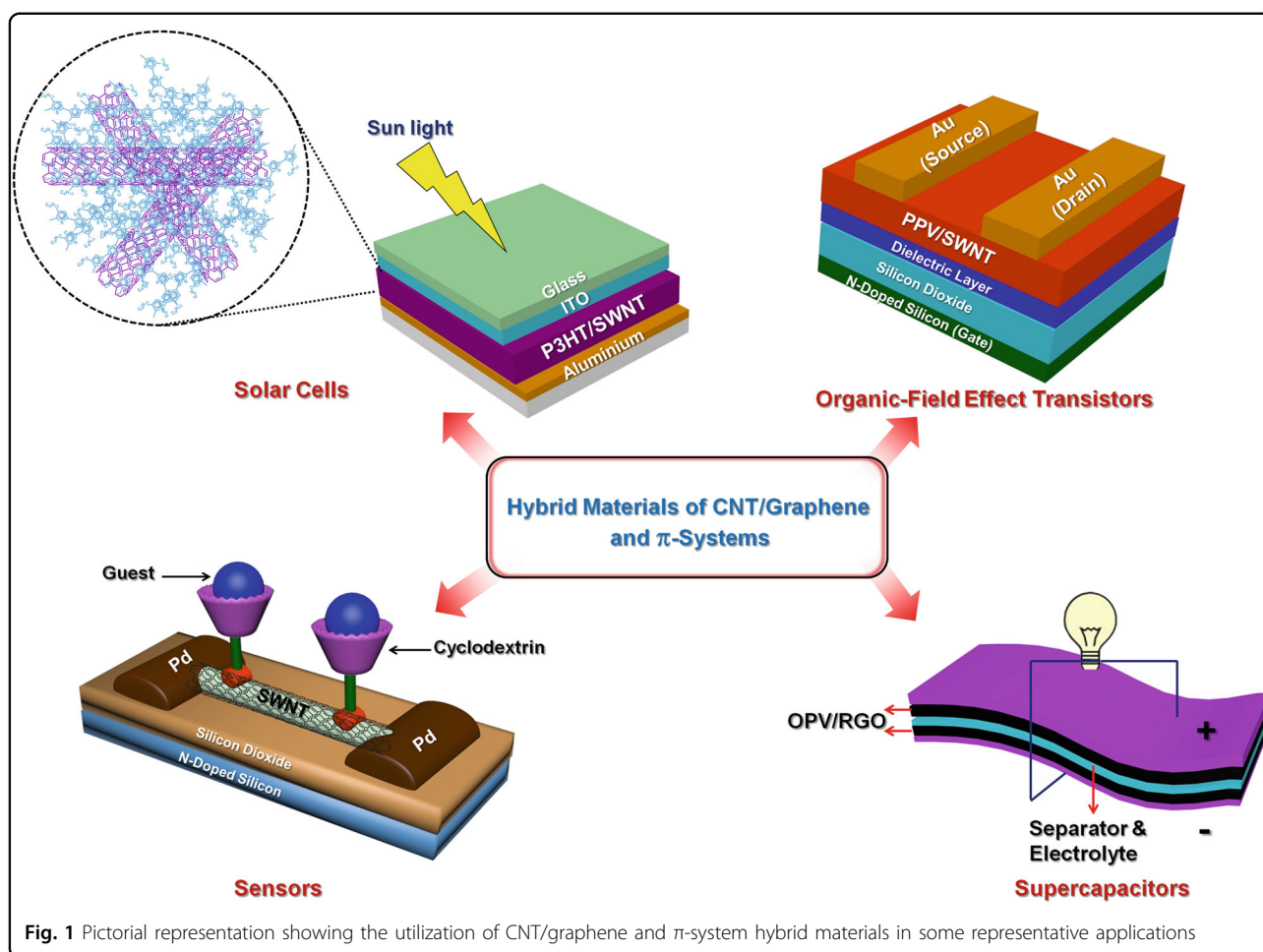


Fig. 1 Pictorial representation showing the utilization of CNT/graphene and π -system hybrid materials in some representative applications

provide an overview and perspective on hybrid materials of 1D and 2D carbon allotropes and synthetic π -systems (Fig. 1) with some illustrative examples.

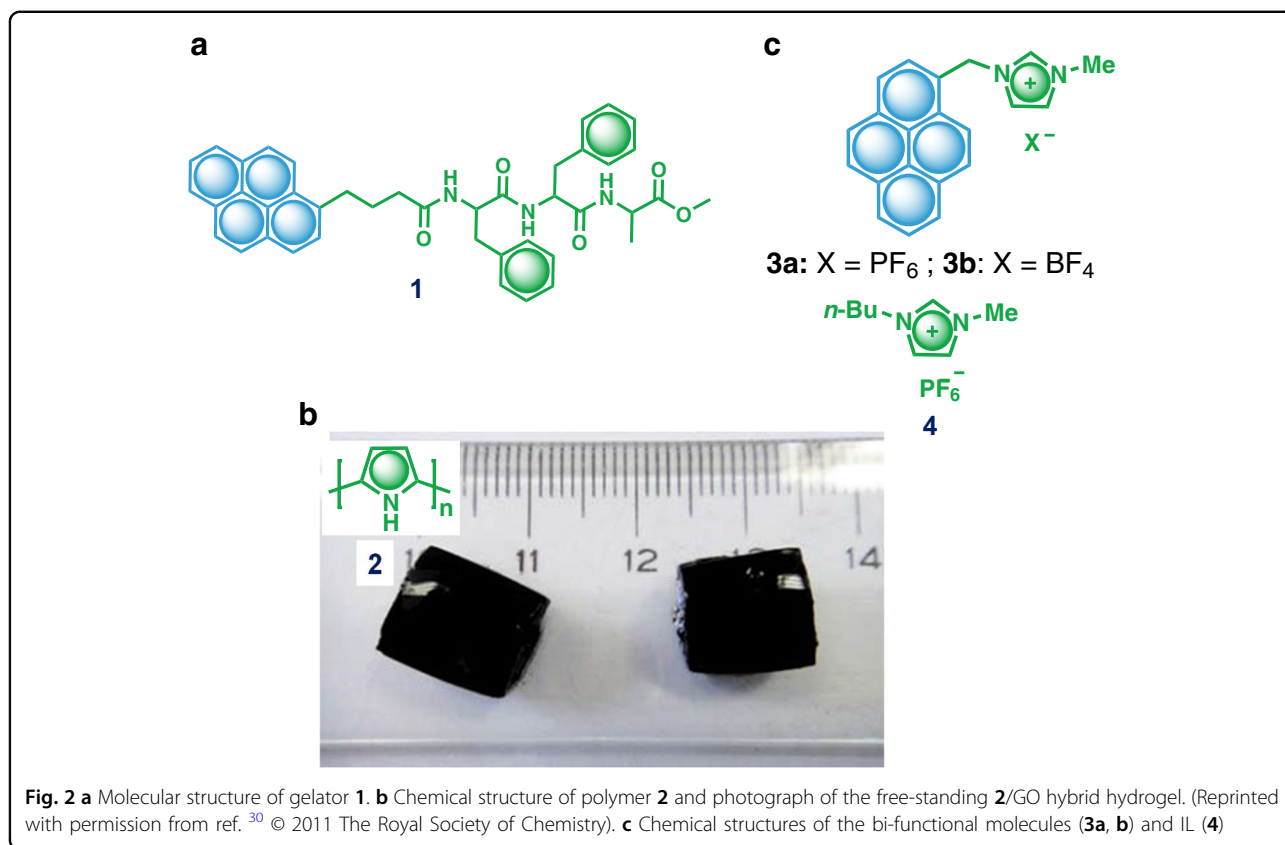
Graphene-based hybrid materials

Graphene is a 2D layered material with extended π -conjugation and unique electronic properties^{20–23}. The extended honeycomb structure of graphene formed through covalent bonding between sp^2 -hybridized carbon atoms gives an exceptional strength-to-weight ratio superior to that of metals and metal-based hybrid materials. Furthermore, the zero electronic band gap in graphene leads to excellent electron mobility and hence make graphene an alternative to the existing semiconductor materials in electronic devices. Graphene derivatives such as GO and RGO possess an atomically thin-layered structure similar to that of graphene but differ in the percentage of oxygen functionalities and sp^2 -hybridized carbon atoms in their basal plane. RGO, which possesses minimal oxygen functionalities and numerous sp^2 -hybridized carbon atoms in its basal plane,

shows electrical properties superior to those of GO. Graphene and its derivatives along with self-assembled organic molecules are applied to the formation of hybrid materials with enhanced electrical and mechanical properties. Both GO and RGO have been successfully incorporated into a variety of supramolecular materials such as gels and assemblies of π -conjugated molecules and polymers^{12,14,24–26}.

Graphene and its derivatives with supramolecular gelators

The interaction of graphene with π -conjugated molecular gelators is a straightforward strategy towards the preparation of hybrid nanostructures. These hybrid gels are mechanically stable and solution processable. There are a few examples of graphene-containing supramolecular gels with improved properties^{27–32}. For instance, it has been shown that graphene could be used as a nucleating surface to reduce the critical gelator concentration of **1** (Fig. 2a)²⁷. Rheological studies have revealed that the rigidity of the hybrid gel (storage



modulus, G') increased sevenfold compared to that of the native gel (Table 1). Hybrid gels prepared by the interaction of GO with conducting polymeric gels have been reported to function as sensors³⁰. A hybrid gel composed of GO and polypyrrole (**2**) prepared by the in situ polymerization of pyrrole in the presence of an aqueous solution of GO (Fig. 2b) has been applied as an ammonia gas sensor owing to its excellent electrical conductivity and electrochemical properties. Upon exposure to ammonia gas (800 ppm) for 600 s, the aerogel prepared by lyophilizing the hydrogel showed a 40% increase in resistance, whereas the corresponding electropolymerized air-dried films displayed marginal changes in resistance (Table 1). This difference in sensing ability was attributed to the intact microstructures of the aerogel that allowed the efficient diffusion of ammonia.

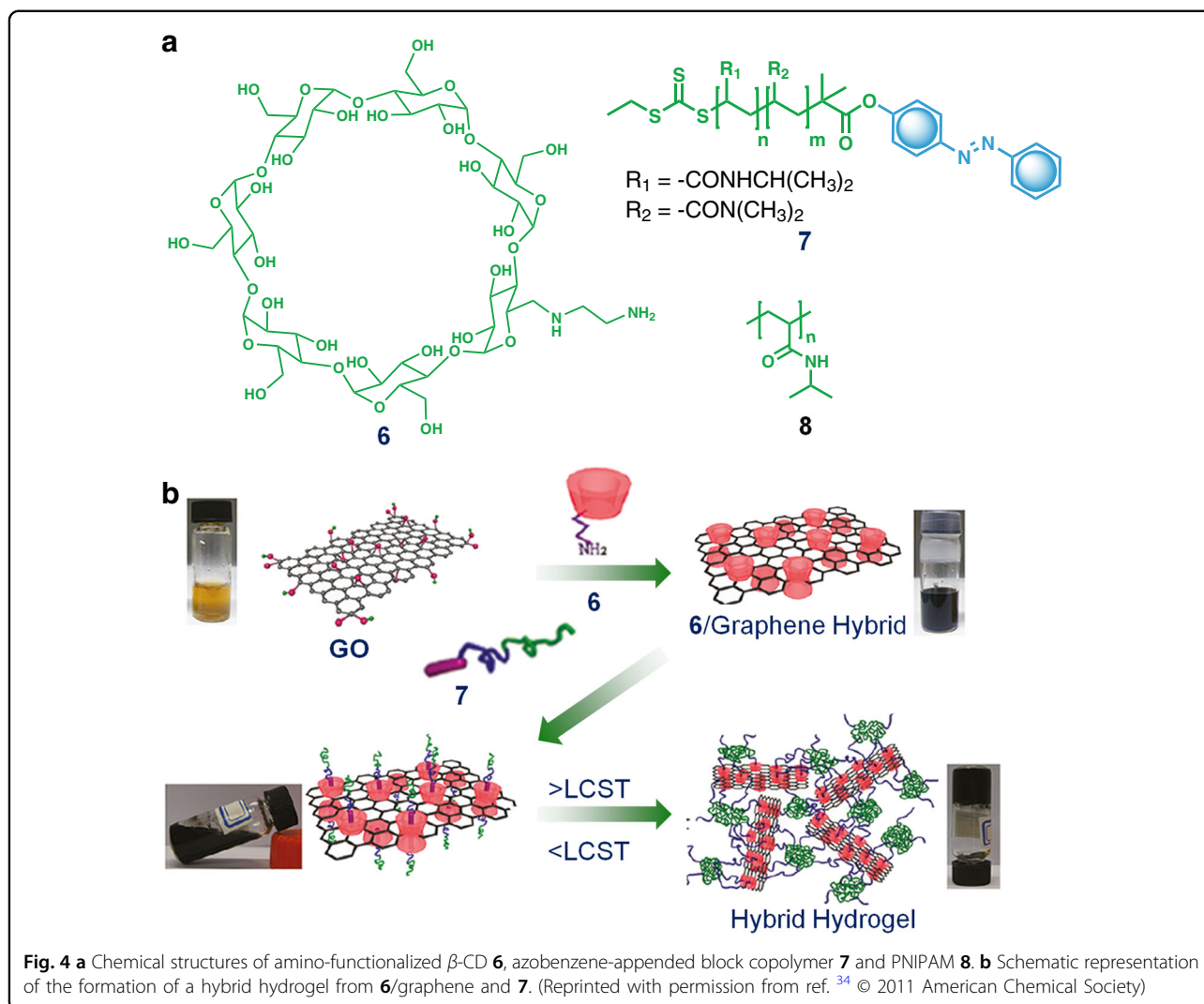
Recently, it has been demonstrated that the ionic liquids (ILs) **3a, b** having pyrene moieties (Fig. 2c) can disperse GO in imidazolium-based ILs through π - π and cation- π interactions³¹. The high-thermal stability and boiling point of ILs allow the thermal reduction of GO to RGO upon heating to 150 °C and the conversion of the dispersion into a gel (Table 1). The IL **4** (Fig. 2c) without pyrene failed to disperse GO even

after sonication for 2 h, corroborating the role of pyrene. Similarly, the counter anions also played a crucial role in the formation and stability of the hybrid gels. The bi-functional molecule **3a** and IL **4** with a larger counter anion, PF_6^- , showed better gelation than **3b** with BF_4^- due to the formation of strong cation- π interactions with thermally reduced GO. In addition to small aromatic molecules, linear π -conjugated molecules have also been used to disperse exfoliated graphene sheets in a gel medium. An oligo (*p*-phenylenevinylene) (OPV)-based gelator, **5**, led to the exfoliation of RGO in nonpolar solvents via noncovalent interactions (Fig. 3a)³². The RGO sheets were found to be highly dispersed due to the presence of self-assembled fibers of **5** on their surface and formed gels at higher concentrations of **5** (Fig. 3b). The exfoliated RGO hybrid exhibited a large surface area and better bulk conductivity than the gel medium alone, leading to its utilization in energy storage applications (Table 1).

Molecular recognition has been widely used to prepare self-assembled hybrids of carbon nanomaterials through complementary host-guest interactions³³. Usually, the host molecules attach to the surface of the carbon materials through covalent or noncovalent functionalization.

Table 1 Comparison of different graphene-based hybrid materials, their synthesis procedure, enhanced properties and applications

Graphene-based hybrid materials	Synthesis procedure	Enhanced property	Application	Ref.
Pyrene-appended tripeptide (1)/ graphene	Sonication (the components are mixed in a suitable solvent and sonicated with heating for few minutes and cooled to rt)	Critical gelation concentration reduced to 0.27% (w/v) from 0.48% (w/v) for native gel and storage modulus of hybrid gel enhanced 7 times	–	27
Polypyrrole (2)/GO hybrid hydrogels	In situ chemical polymerization	Low critical gel concentration (<1% by weight), high storage moduli (> 10 kPa) and electrical conductivity	Ammonia gas sensing as low as 800 ppm	30
Pyrene-functionalized ILs (3a , b)/ RGO hybrid gels	Thermal reduction at 150 °C	Retains gel-like nature up to 46% of applied strain amplitude	Energy storage devices	31
OPV (5)/RGO hybrid	Chemical reduction (NaBH ₄)	Increased gel melting temperature and conductivity (6.3 S m ⁻¹)	Electrodes for double layer supercapacitors (C _{sp} —181 Fg ⁻¹ at current density of 1 Ag ⁻¹)	32
β -CD functionalized RGO (6)/PDMA- <i>b</i> -PNIPAM block copolymer (7)	Thermal reduction at 80 °C	Enhanced sol-gel thermo-reversibility	Drug delivery and tissue scaffolds	34
1-Pyrene-carboxylic acid (9)/ exfoliated graphene from graphite	Sonication	Up to 6% CO ₂ can be detected	Gas sensor and supercapacitor (C _{sp} —120 Fg ⁻¹)	36
1-Pyrene-sulfonate (12)/RGO	Chemical reduction (NH ₂ NH ₂ ·H ₂ O) at 80 °C	Electrical conductivity of 916 S m ⁻¹ with a transmittance of 68%	Anode material for bulk-heterojunction solar cells	41
Cationic porphyrin (14)/RGO	Chemical reduction (NH ₂ NH ₂ ·H ₂ O) at 95 °C	Optical detection of Cd ²⁺ (~0.1 μM)	Metal ion sensor	42
Anionic copper phthalocyanine (16)/graphene	Sonication	Decreased in vitro cancer cell viability from 68 to 29%	Photodynamic and photothermal therapy (cancer theranostics)	44
PPE-SO ₃ Na (18)/RGO	Chemical reduction (NH ₂ NH ₂ ·H ₂ O) at 80 °C	Improved water dispersibility and stability	Conducting material for optoelectronic devices	46
Polypyrrole (2)/GO	In situ emulsion polymerization	Improved electrical conductivity (5 S m ⁻¹) than polypyrrole (0.94 S m ⁻¹) and GO (1 × 10 ⁻⁶ S m ⁻¹)	Molecular electronics	50
P3HT (21)/isocyanate-derived GO	Chemical treatment of GO with phenyl isocyanate	Power conversion efficiency of 1.1% with an open-circuit voltage of 0.72 V	BHJ solar cells	52
PEDOT (22)/RGO	Chemical reduction (NH ₂ NH ₂ ·H ₂ O) of GO on a glassy wafer in vapor state	Twofold enhancement in electrical conductivity and sixfold improvement in mechanical strength	Optoelectronic devices	54

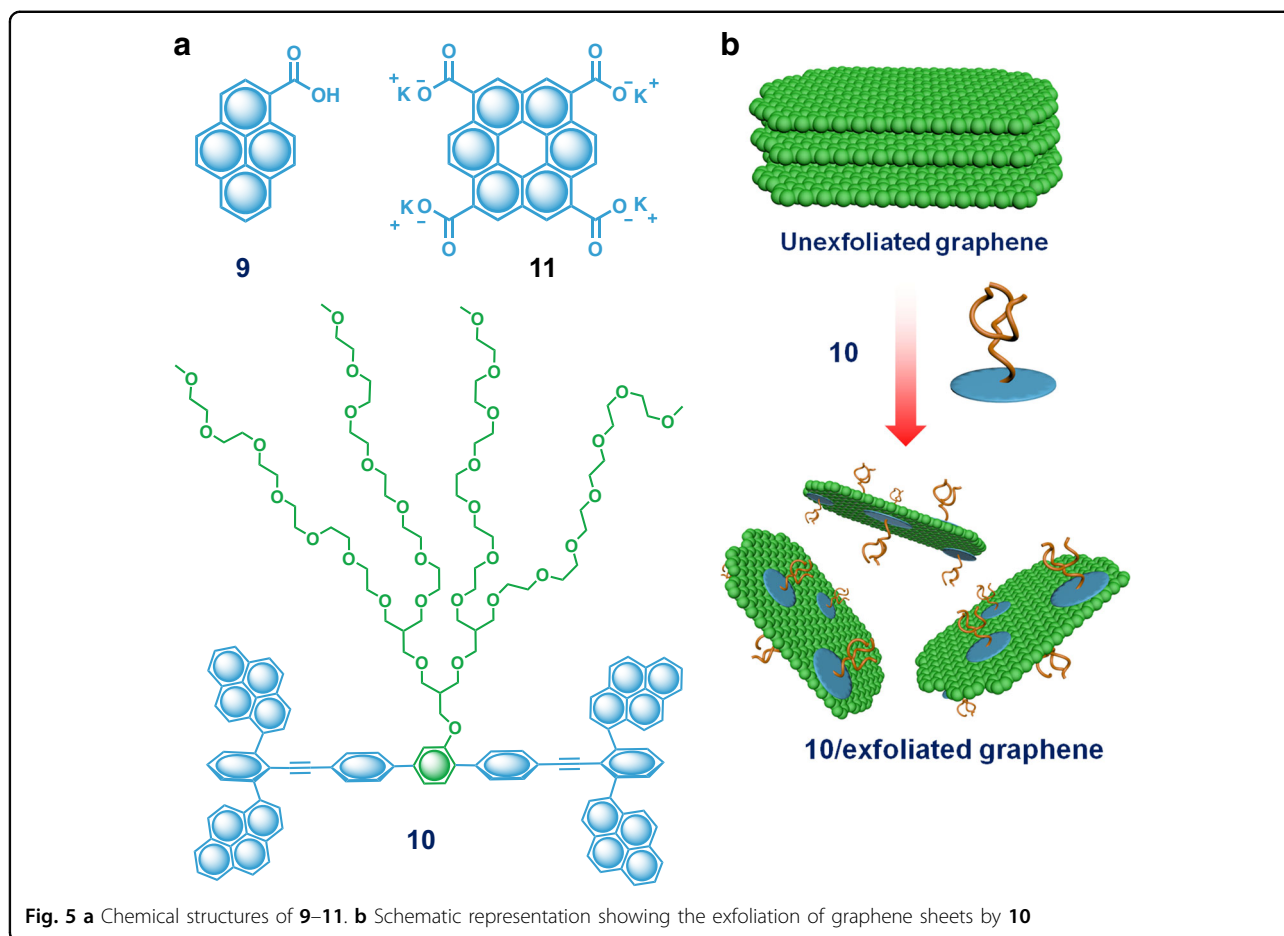


hindered its effective interactions with the curved surface of single-walled nanotubes (SWNTs), leading to its selectivity towards graphene. A coronene carboxylate, **11** (Fig. 5a), has also been used for the noncovalent functionalization and solubilization of graphene from graphite in water and showed better interactions with graphite than with GO⁴⁰. The strong charge transfer and π - π interactions between negatively charged **11** and graphite produced stable dispersions of exfoliated graphene sheets in water.

The noncovalent functionalization of RGO with aromatic donor and acceptor molecules has resulted in hybrid materials with tunable electronic properties. For example, the interaction of the sodium salt of 1-pyrene sulfonic acid, **12** (donor), and the disodium salt of the bis-benzenesulfonic acid, **13** (acceptor, Fig. 6), with graphene-produced water-soluble hybrid materials⁴¹. While the aromatic molecules exhibited strong π -interactions with

graphene sheets, the negatively charged molecules prevented aggregation, leading to a stable dispersion of the hybrid material in solution. Upon thermal reduction at higher temperatures in the presence of Ar and H₂, these hybrid materials exhibited conductivity values of 1149 and 1314 S cm⁻¹, respectively, whereas pristine RGO exhibited a much lower value of 517 S cm⁻¹. The observed enhancement in conductivity of the hybrid materials is attributed to the better graphitization and deoxygenation of the basal plane of RGO. Furthermore, these hybrid materials showed a better power conversion efficiency than pristine RGO when used as an electrode material in bulk-heterojunction solar cells (Table 1).

The water-soluble cationic porphyrin **14** (Fig. 6)⁴² and the sulfonate-functionalized and quaternary ammonium group-functionalized porphyrins **15a** and **15b**, respectively (Fig. 6)⁴³, were used to prepare hybrid materials with RGO. The electrostatic and π - π interactions



between positively charged **14** and negatively charged graphene sheets resulted in the flattening of **14**, leading to enhancements in the π -conjugation and electron-withdrawing effects (Fig. 6). The **14**/RGO hybrid was used for rapid and selective detection of Cd^{2+} in aqueous media via accelerated coordination reaction between **14** and Cd^{2+} in the presence of RGO sheets (Table 1). While **15a** self-assembled on the surface of graphene via π - π interactions, the electrostatic repulsion between the negative charges ensured the stability of the aqueous dispersion. A thin film of this hybrid material exhibited an 80% optical transparency and an electrical resistance of $5 \text{ K}\Omega \text{ m}^{-1}$. In another report, a hybrid material composed of graphene and an anionic phthalocyanine, **16**, (Fig. 6) in water was employed as a photosensitizer and a photothermal therapeutic agent, which showed excellent anticancer efficacy (Table 1)⁴⁴.

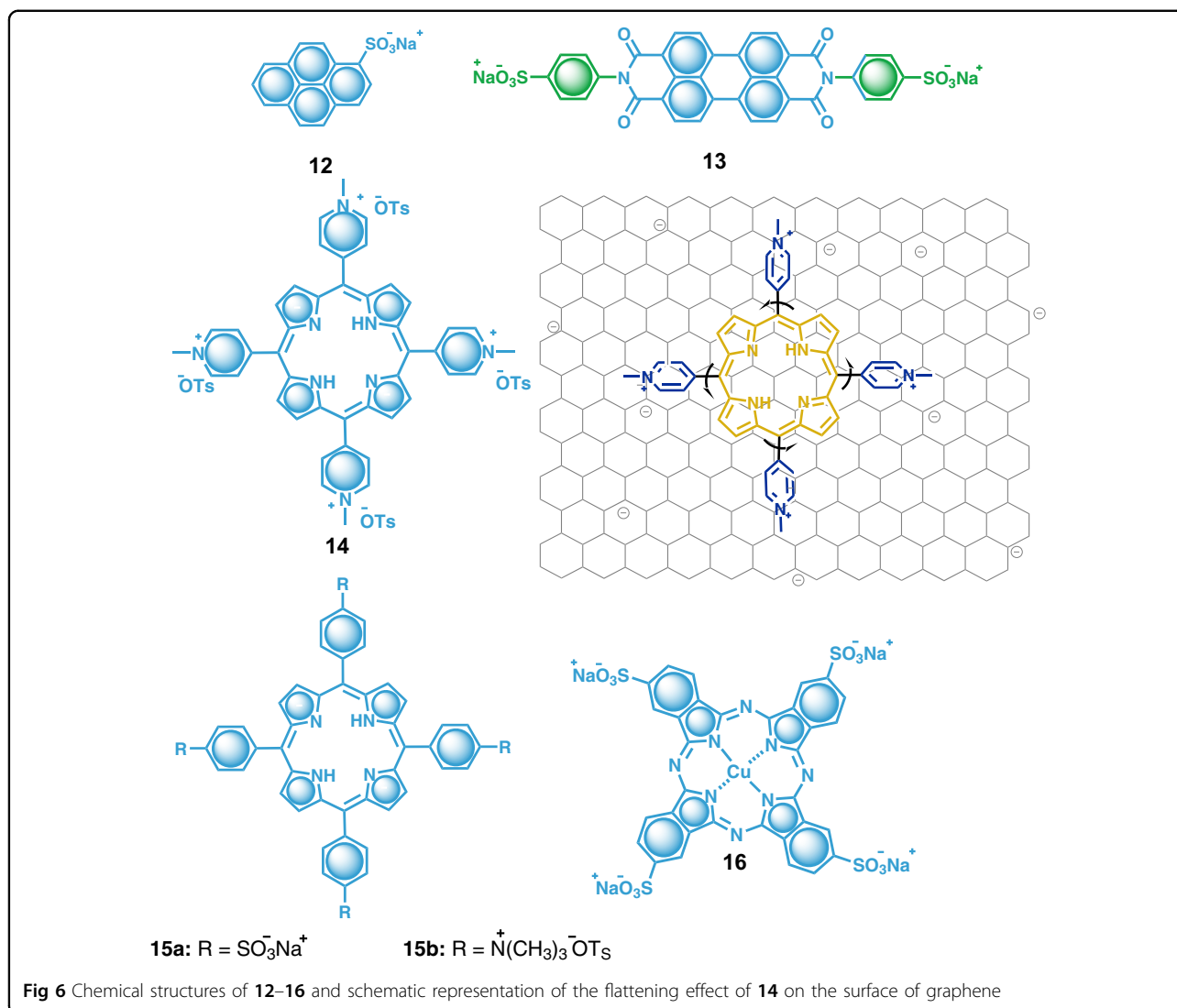
Graphene and its derivatives with π -conjugated polymers

π -conjugated polymers are known to interact with graphene through noncovalent interactions. Hybrid

materials of RGO and π -conjugated polymers such as poly(*p*-phenylenevinylene)⁴⁵, poly(*p*-phenyleneethynylene)⁴⁶, polyaniline^{47–49}, and polypyrrole⁵⁰ have found applications in solar cells as well as in optoelectronic devices such as field-effect transistors and sensors.

A hybrid material of the polymer **17** (Fig. 7) and RGO has been reported for studying the mechanism of energy transfer between donor and acceptor systems via time-resolved fluorescence dynamics⁴⁵. Polymer **17** showed a fluorescence lifetime of 200 ps that, however, showed a faster decay in the presence of 50% RGO due to energy transfer from the polymer to RGO. A hybrid of a conjugated polyelectrolyte, **18** (Fig. 7), and graphene was reported to exhibit a low resistance of $30 \text{ K}\Omega$ and found applications in optoelectronic devices (Table 1)⁴⁶.

A hybrid composed of GO and polyaniline **19** (Fig. 7) was prepared via mild oxidation of aniline with a mixture of H_2O_2 , HCl, and $\text{FeCl}_3 \cdot 6\text{H}_2\text{O}$ in the presence of various amounts of GO⁴⁷. The charge storage capacity of **19** increased considerably with a minimum weight % of GO. A similar kind of hybrid material was also prepared by

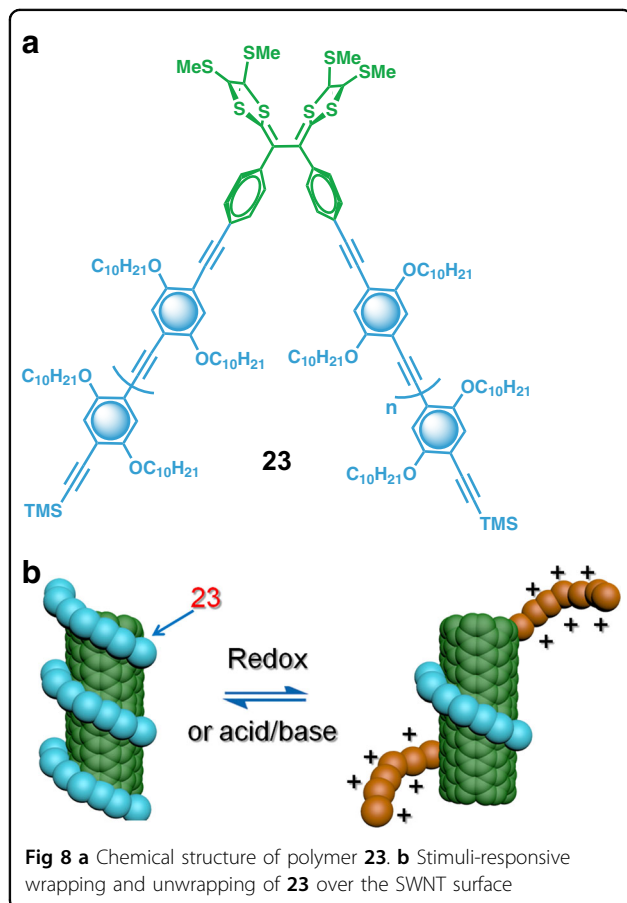
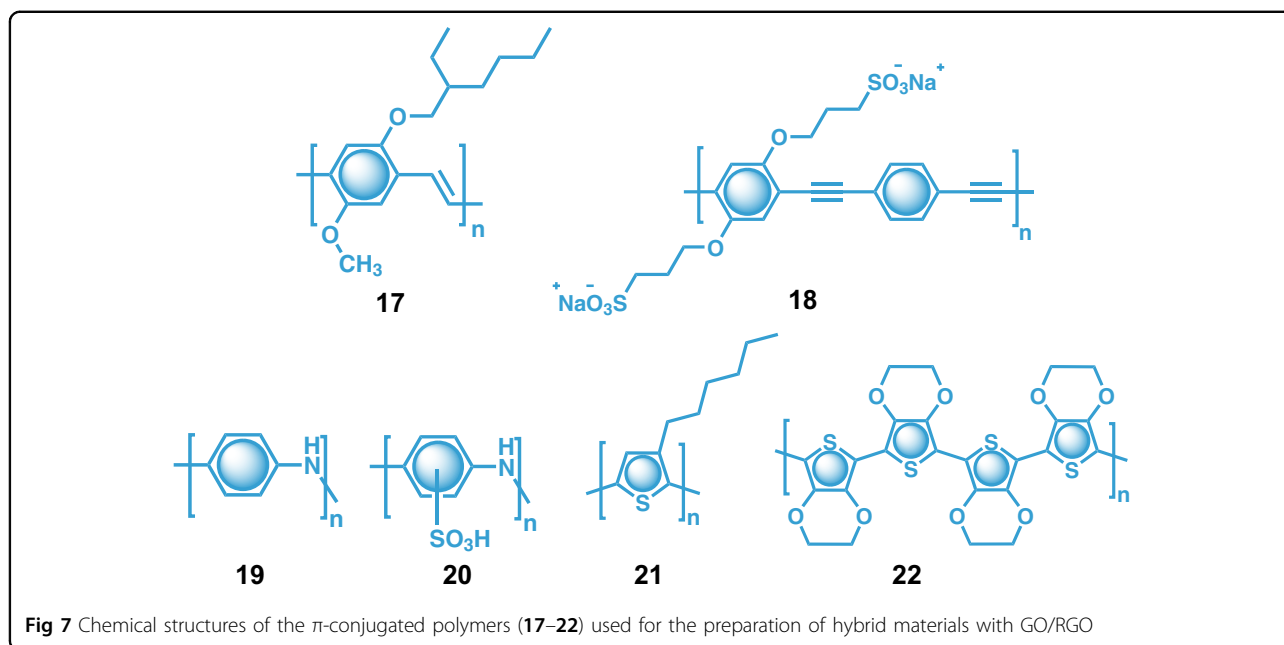


in situ polymerization of aniline in the presence of GO followed by reduction using hydrazine hydrate⁴⁸. Morphological studies revealed the presence of nanofibrous structures of **19** on the surface of the graphene sheets. The **19**/RGO hybrid exhibited a higher conductivity and charge storage capacity than **19**. A sulfonated polyaniline, **20** (Fig. 7), was reported to form a highly water-soluble ($>1 \text{ mg mL}^{-1}$) electroactive hybrid material with RGO that exhibited a conductivity of 0.3 S m^{-1} in the film state⁴⁹.

Hybrid materials of polypyrrole **2** and GO were prepared by emulsion polymerization of pyrrole in the presence of multi-layered graphite oxide (an oxidized form of bulk graphite)⁵⁰. The π - π interaction-mediated self-assembly of **2** on the surface of the unoxidized domains of GO in the multi-layered graphite oxide led to delamination of the latter into individual GO sheets in water. The

electrical conductivity of the **2**/GO hybrid material was reported to be 5 S cm^{-1} , whereas **2** and GO exhibited low conductivity values of 0.94 and $1 \times 10^{-6} \text{ S cm}^{-1}$, respectively (Table 1).

To exploit the excellent electronic properties of graphene as an acceptor in bulk-heterojunction organic solar cells, a few graphene-based hybrid materials with poly(3-hexylthiophene) (P3HT, **21**)^{51,52} and poly(3,4-ethylenedioxy-thiophene) (PEDOT, **22**) (Fig. 7) were investigated^{53,54}. For instance, a hybrid material composed of **21** and functionalized graphene (0–15%) was tested for solar cell applications⁵². Photovoltaic devices fabricated with this hybrid material exhibited a power conversion efficiency of 1.1% with an open-circuit voltage of 0.72 V (Table 1). Hybrid materials composed of RGO and **22** were used as transparent electrode materials for optoelectronic devices⁵³. A hybrid film of **22**/RGO



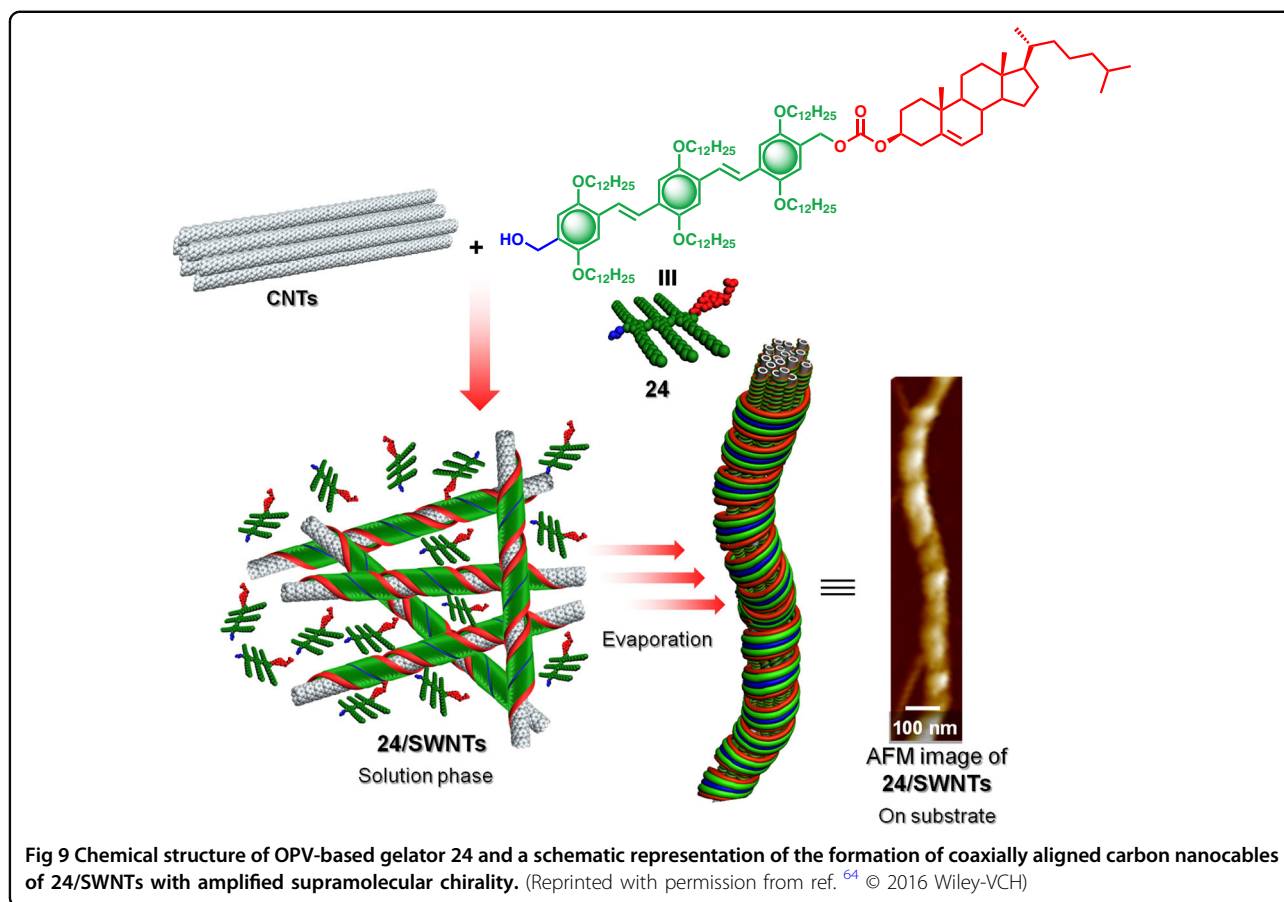
exhibited an electrical conductivity of $\sim 0.2 \text{ S cm}^{-1}$ and an 88% transmittance in the range 400–1800 nm. The hybrid materials of RGO with **22** as double-layered (**22**/graphene) and triple-layered (graphene/**22**/graphene) films ($\sim 32 \text{ nm}$ thick) exhibited conductivity values of 13 and 12 S cm^{-1} , respectively⁵⁴. Furthermore, free-standing films made of these hybrid materials were 91% optically transparent and exhibited a sixfold enhancement in the mechanical strength relative to that of the pristine films (Table 1). These exceptionally conductive, transparent, and free-standing films with superior mechanical strength were explored for potential applications in optoelectronics and sensing. All the details of the synthetic routes, properties and applications of graphene-based hybrid materials are summarized in Table 1.

Carbon nanotube-based hybrid materials

CNTs are an allotrope of carbon with a 1D nanotubular structure and are broadly classified as SWNTs, double-walled, and multi-walled nanotubes (MWNTs)^{11,23}. The electrical conductivity of CNTs ranges from metallic to semiconducting based on the diameter and the rolling angle, which also impart chirality in the tubes¹¹. CNTs have excellent chemical, mechanical, and electronic properties that make them promising for various applications. The noncovalent functionalization of CNTs with aromatic molecules and π -conjugated polymers has been extensively investigated^{11–14,55–62}. The surface modification of CNTs through noncovalent interactions improves their dispersion and solution processability, rendering them suitable for device applications.

Table 2 Comparison of various CNT-based hybrid materials, their synthesis procedure, enhanced properties and applications

Carbon nanotubes based hybrid materials	Synthesis procedure	Enhanced property	Application	Ref.
TFV-phenylacetylene foldamer (23)/SWNTs	Sonication and centrifugation	Tube diameter-dependent wrapping of foldamer	Separation of specific SWNTs	63
Cholesterol appended OPV (24)/CNTs	Sonication	Formation of super-helical coaxial nanocables with amplified supramolecular chirality of OPV	–	64
Squaraine dye (25)/SWNTs	Sonication	Ultrasound-induced gelation of squaraine dye at relatively low concentration (2 mM) in presence of SWNTs	–	67
β -CD-Ru complex (26)/pyrene-adamantane (27)/SWNTs	Grinding in solid state followed by sonication in aqueous solution	Spatial controllable DNA condensation	Non-viral gene delivery system	72
Amphiphilic PDI (29)/SWNTs	Sonication and centrifugation	Tube diameter-dependent side-wall functionalization of SWNTs	Separation of specific SWNTs	73
Tweezer-shaped PDI (30)/HIP-co-SWNTs	Sonication and centrifugation	Selective dispersion of SWNTs with diameter > 0.8 nm	Separation of specific SWNTs	75
Amphiphilic PDI (31)/SWNTs	Sonication	Low resistivity of hybrid film	Size-selective separation of gold nanoparticles	76
OPV (33)/MWNTs	Sonication	Greater water contact angle of $\sim 165^\circ$ (OPV $\sim 106^\circ$, MWNTs $\sim 128^\circ$)	Self-cleaning and smart surfaces	77
OPEs with complementary H-bonding moieties (34a, b and 35)/MWNTs	Sonication and filtration	Reversible solubilization of MWNTs through complementary H-bonding	–	78
Imidazolium ion-appended triphenylene derivative (37)/SWNTs	Heating at 150 °C followed by grinding for 30 min	Alignment of SWNTs, anisotropic electrical conductivity	–	80
PPV (39a, b)/SWNTs	Sonication	Solubilization of SWNTs by wrapping of conducting polymers	Molecular actuators and switches	86
PPE (40)/HIP-co-SWNTs	Sonication	Helically wrapped SWNTs (pitch length ~ 13 nm)	–	87
P3HT (21)/SWNTs	Sonication	Free-standing, conductive, transparent hybrid film	Bulk-heterojunction solar cells	90
Chiral binaphthol-fluorene copolymers (48a, b)/CoMoCAT-SWNTs	Sonication and centrifugation	Extraction of either right-handed or left-handed SWNTs	Separation of specific SWNTs	92
Pyrene-appended poly(phenylene acetylene) (49)/MWNTs	Sonication	Bipolar photovoltaic cells	Optoelectronic devices	93



Carbon nanotubes and supramolecular gelators

The solution processability of CNTs can be enhanced by incorporating them into supramolecular gel matrices. For instance, the phenylacetylene polymer **23** (Fig. 8a) interacted with HiPco-SWNTs in toluene to form a hybrid gel⁶³. The wrapping and unwrapping of **23** over the SWNT surface could be controlled by an electrochemical redox response (Fig. 8b). This gelation process did not occur with CoMoCAT-SWNTs due to the inability of **23** to adhere to the surface of SWNTs having a small diameter. This selective interaction of **23** with SWNTs was exploited to chirally enrich a mixture of SWNTs with multiple chiral structures (Table 2).

OPV-based gelators have been shown to interact strongly with SWNTs and MWNTs through π -stacking interactions to form stable hybrid gels in nonpolar solvents⁵⁵. The interaction of OPVs with CNTs leads to debundling of the nanotubes, and the specific arrangement of the debundled SWNTs/MWNTs and **24** reinforces the supramolecular fibrous structures (Fig. 9). This strong π - π interaction of OPVs with SWNTs was exploited to facilitate the self-assembly of a chiral π -gelator, **24**, resulting in the amplification of chirality

even at low concentrations⁶⁴. The OPV **24** with amplified chirality in the presence of SWNTs showed distinct morphological features, such as coaxially aligned carbon nanocables in which each SWNTs were helically wrapped with the gelator (Table 2).

Host-guest interactions between photoresponsive polymers containing azobenzene moieties and SWNTs have been successfully utilized to form stimuli-responsive hybrid hydrogels^{65,66}. In another report, a supramolecular hybrid gel composed of a squaraine derivative, **25**, and SWNTs was prepared through ultrasonic irradiation (Fig. 10)⁶⁷. Upon sonication, the self-assembly of **25** resulted in the formation of entangled fibrous structures leading to gelation. Furthermore, the rate of nucleation and growth of the self-assembled structures could be enhanced by introducing heterogeneous nucleation sites by adding very small amounts of SWNTs to an *n*-butanol solution of **25** at concentrations less than the critical gelation concentration (Table 2). Morphological analyses revealed that the ultrasound-induced self-assembly of **25** led to crystalline fibrous structures, whereas in the presence of SWNTs, the same process led to a nanotape-like morphology (Fig. 10b). Intermolecular H-bonding,

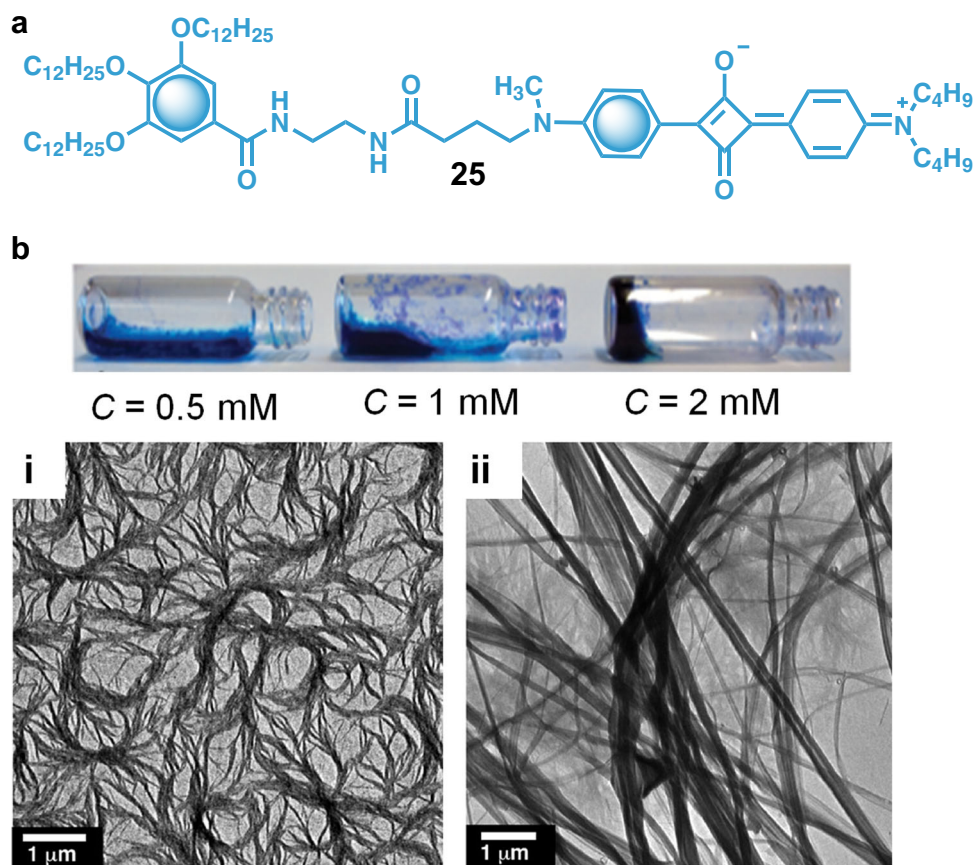


Fig 10 a Chemical structure of the squaraine dye-derived gelator **25**. b Photographs of **25** in *n*-butanol with 0.1 mg of SWNTs after sonicating for 5 min. Transmission electron microscopy images of (i) **25** gel and (ii) **25**/SWNT gel (*n*-butanol, 2 mM). (Reprinted with permission from ref. ⁶⁷ © 2013 Wiley-VCH)

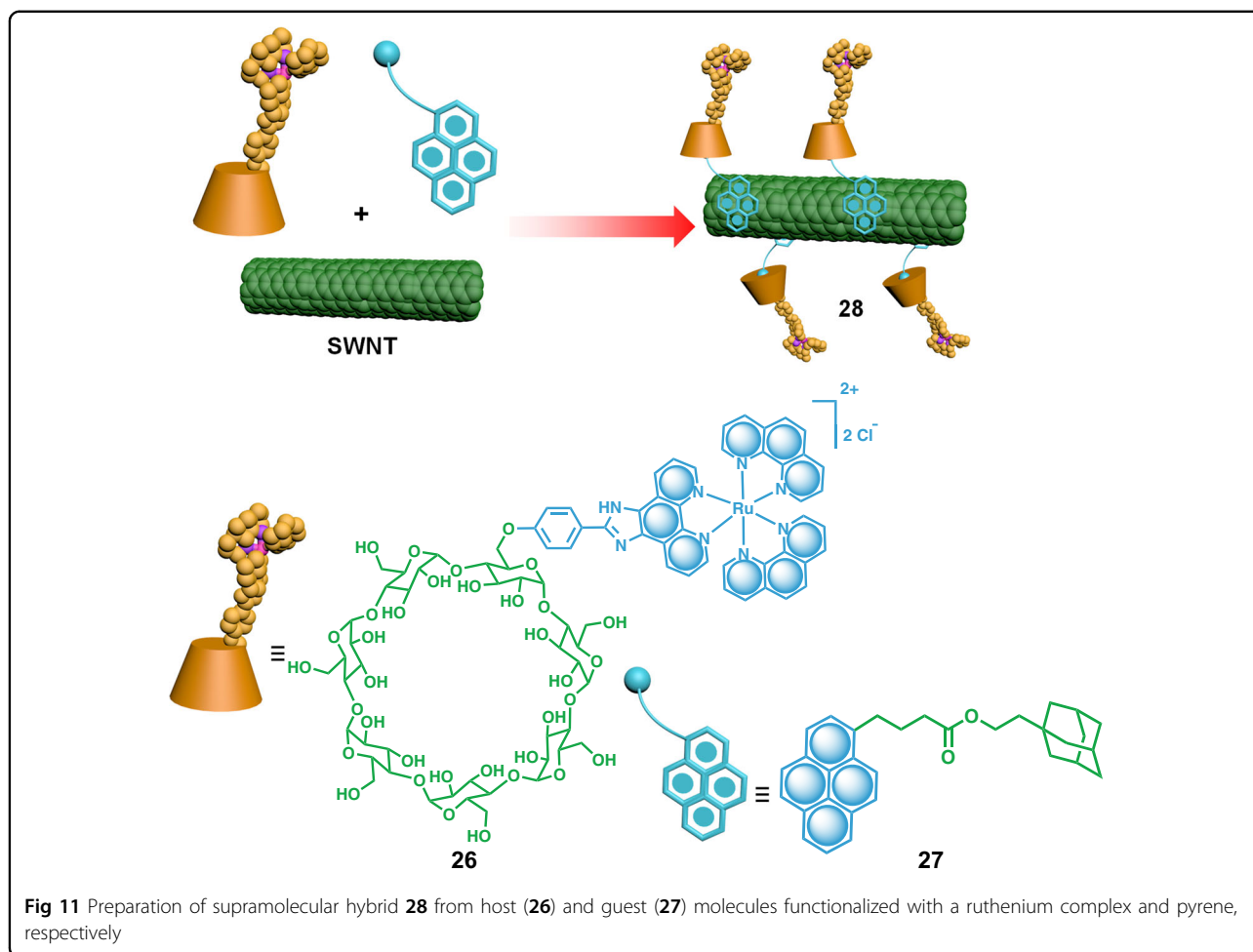
π -stacking, and hydrophobic interactions were responsible for the sonication-induced formation of crystalline fibers of **25**. However, the heterogeneous nucleation and growth of **25** on the SWNT surface via π -stacking and H-bonding resulted in a less crystalline nanotape-like morphology.

CNTs and π -conjugated supramolecules

Due to their extended π -surfaces, polyaromatic molecules such as naphthalene, anthracene, pyrene, and perylene have been used extensively to prepare hybrid materials with CNTs^{11–14,68–71}. Supramolecular systems of these molecules have been exploited in the preparation of hybrid materials with CNTs. For instance, a supramolecular SWNT hybrid (**28**) composed of a ruthenium complex tethered to β -CD, **26**, and a pyrene-functionalized adamantane, **27**, were prepared by mixing the three components (**26**, **27**, and SWNTs) in the solid state (Fig. 11)⁷². The finely ground solid was then dispersed in 0.01 M NaOH by

sonication, and the interactions between the components were studied by various analytical techniques. The appearance of van Hove singularities in the absorption spectra indicated that the dispersion of SWNTs in water occurred via π - π interactions between the pyrene of **27** and the SWNTs. The fluorescence intensity of ruthenium complex **26** was quenched due to the photoinduced charge transfer process arising from the close proximity of the SWNTs and **26**. The cationic supramolecular hybrid **28** was further functionalized with DNA and used for non-viral gene delivery applications (Table 2).

A water-soluble perylene diimide (PDI) dye, **29**, functionalized with Newkome-type dendritic moieties (Fig. 12) was also used to disperse SWNTs in water^{73,74}. The polar carboxyl groups led to enhanced water solubility, and the nonpolar perylene moiety facilitated the dispersion of SWNTs. Absorption spectroscopy revealed that 0.01 wt% of **29** was enough to stabilize the dispersion. The fluorescence of



molecule **29** was quenched in the hybrid, indicating the possibility of photoinduced electron/energy transfer from **29** to the SWNTs. The tweezer-shaped molecule **30** with two PDI units (Fig. 12) facilitated the sorting of SWNTs based on their diameters⁷⁵. This molecule was not only used to disperse SWNTs but also to enrich (up to 70%) the as-produced HiPco-SWNTs having a diameter of 0.8 nm (Table 2). Furthermore, the PDI-based amphiphiles **31** and **32** (Fig. 12) were also found to disperse SWNTs in organic and aqueous media⁷⁶. Detailed morphological studies revealed the monolayer absorption of **31** and **32** on the SWNTs in chloroform, and a helical assembly of **31** was formed over the SWNTs in water due to hydrophobic and π -stacking interactions. Transient absorption spectroscopy indicated that a rapid photoinduced electron transfer occurs from SWNTs to **31** upon excitation. The composite of **31**/SWNTs forms a porous supramolecular membrane, which was used to separate 2–6 nm-sized gold nanoparticles from a mixture having different sizes (Table 2). In addition,

the hybrid materials of **31**/SWNTs were utilized to prepare bucky paper for electronic applications.

Furthermore, OPV **33** (Fig. 13a) was reported to interact with SWNTs and MWNTs to form uniform dispersions in nonpolar solvents such as *n*-hexane and *n*-decane⁷⁷. Molecule **33** self-assembled over the π -surface of the MWNTs, leading to a wax-like coating (Fig. 13b). Morphological analysis of the hybrid material revealed the presence of nanoscopic and microscopic architectures, as seen in natural superhydrophobic surfaces like lotus leaves. The hybrid material exhibited a water contact angle of 165° with self-cleaning properties (Fig. 13c, d) and was stable under acidic and basic conditions (Table 2).

The reversible noncovalent functionalization of MWNTs was demonstrated using oligo(*p*-phenyleneethynylene)s (OPEs) (**34a**, **b** and **35**) with complementary H-bonding moieties (Fig. 14a)⁷⁸. The π - π and CH- π interactions present between the MWNTs and OPEs resulted in wrapping of the H-bonded supramolecular polymer over the graphitic surface of the MWNTs,

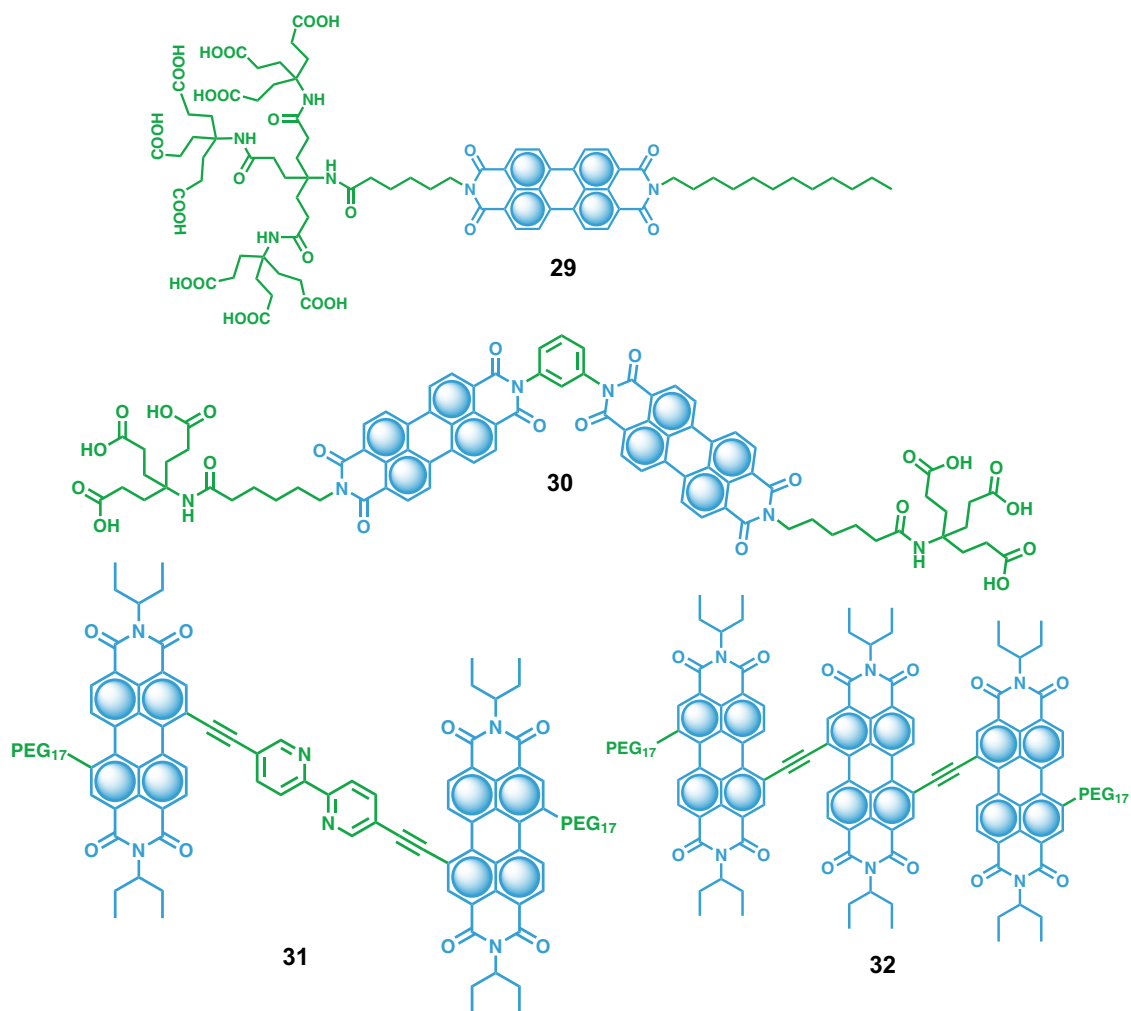


Fig 12 Chemical structures of the PDI-based molecules **29–32** used for the preparation of hybrid materials with SWNTs

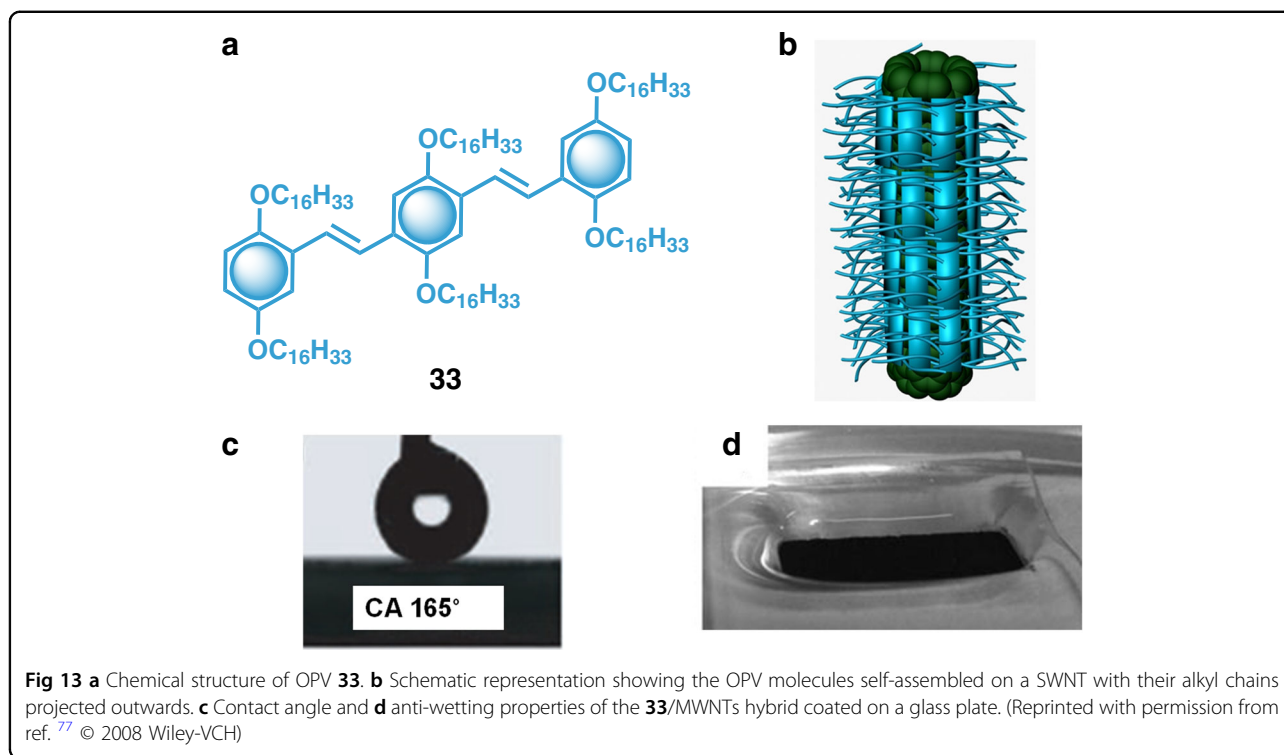
leading to the solubility of the MWNTs in nonpolar solvents. The reversibility of MWNTs solubilization was investigated by adding polar/protic solvents that perturbed the H-bonding interactions between the OPE molecules via partial detachment of the wrapped molecules followed by the precipitation of MWNTs. In addition to chemical stimuli, the role of light in the reversible solubilization of nanotubes was also studied by introducing light-sensitive azobenzenes into the OPE backbone of **36** (Fig. 14b)⁷⁹. The proper orientation of the OPE molecules for better interactions with the MWNTs was achieved by the *cis/trans*-isomerization of the azobenzenes attached to the molecule, eventually leading to the iterative solubilization and precipitation of MWNTs (Table 2).

A triphenylene-based ionic liquid crystalline (LC) molecule (**37**) was capable of dispersing SWNTs in a

columnar LC phase (Fig. 15a)⁸⁰. The dispersed SWNTs forced the LC columns to orient in the macroscopic length scale. The LC columns and dispersed SWNTs adopted three different orientations with respect to each other: random, homeotropic, and horizontal (Fig. 15b). The alignment of the SWNTs was found to be retained for a long period, which makes the SWNT–LC hybrid materials potential candidates for anisotropic electrical conductors (Table 2).

CNTs and π -conjugated polymers

π -conjugated polymers interact strongly with CNTs due to their extended π -surfaces and large area of contact between them⁸¹. A large number of polymers such as poly(*p*-phenylenevinylene) (PPV), poly(*p*-*m*-phenyleneethynylene) (PPE), poly(9,9-dialkylfluorene), and poly(3-alkylthiophene) have been reported to form self-

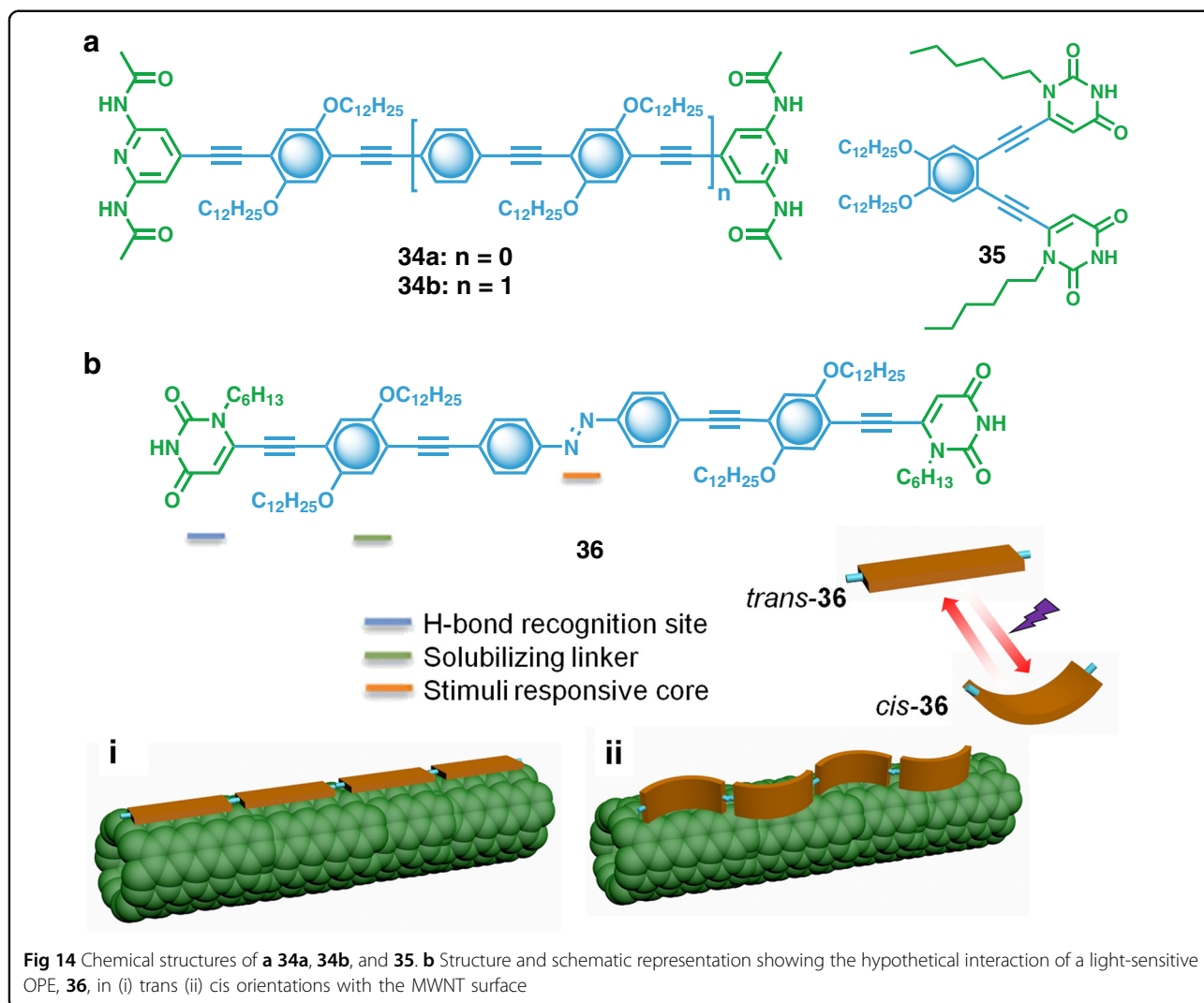


assembled hybrids with CNTs^{81–84}. Polymer **38** (Fig. 16a) formed hybrid materials with SWNTs via helical wrapping of individual or bundles of nanotubes⁸⁵. The formation of the fibrous network structure by wrapping of the bundles containing a few SWNTs rather than the aggregation of individually wrapped SWNTs was confirmed by microscopic analysis. Theoretical studies predicted the parallel arrangement of **38** over the π -surface of the bundled SWNTs through strong supramolecular interactions. Polymers **39a** and **39b** (Fig. 16a) were used to prepare hybrid materials of polypseudorotaxanes with SWNTs⁸⁶. These hybrid materials may find applications as molecular actuators and switches with improved properties (Table 2).

Similar to PPVs, PPEs have also been found to facilitate the dispersion of SWNTs in both aqueous and organic solvents. For example, the size-selective dispersion of SWNTs of a particular chirality was achieved using polymer **40** (Fig. 16b)⁸⁷. Absorption and fluorescence studies showed that the aqueous dispersion of **40**/SWNTs exclusively contained small-diameter nanotubes such as (6, 5; $d = 0.757$ nm) and (8, 3; $d = 0.782$ nm), whereas the large diameter ones ((7, 5), (8, 4), and (7, 6); $d = 0.829$, 0.840, and 0.895 nm) were removed from the as-synthesized SWNTs samples by centrifugation. The rotation around the $-C\equiv C-$ bonds of the

phenyleneethynylene unit of **40** played a crucial role in the helical wrapping of SWNTs having a definite chirality. Theoretical calculations indicated that the size of the cavity formed via the helical arrangement of **40** was most suited to SWNTs with diameters of 0.757–0.782 nm (Table 2). A series of PPEs, **41–43** (Fig. 16b), were used for dispersing as-synthesized SWNTs in organic solvents through noncovalent interactions⁸⁸. Polymer **41** showed a poor dispersion ability towards raw SWNTs, whereas polymers **42** and **43** with longer conjugation lengths afforded stable dispersions in organic solvents. The appearance of van Hove singularities in the absorption spectra and the quenching of the fluorescence of **42** and **43** indicated that the dispersion of the debundled SWNTs occurred via a self-assembly process. A water-soluble polymer, **44** (Fig. 16b), was also utilized to disperse SWNTs in an aqueous medium⁸⁹. Absorption spectroscopy and atomic force microscopy analysis confirmed the individualization of the SWNTs and the helical self-assembly of **44** over the π -surface of the SWNTs.

A lightweight, transparent, and highly conductive thin film for optoelectronic applications was prepared from a hybrid material comprising P3HT, **21** (Fig. 7) and SWNTs (Table 2)⁹⁰. The thickness of the film could be tuned by adjusting the dispersion concentration of the hybrid material. Furthermore, the hybrid films could be

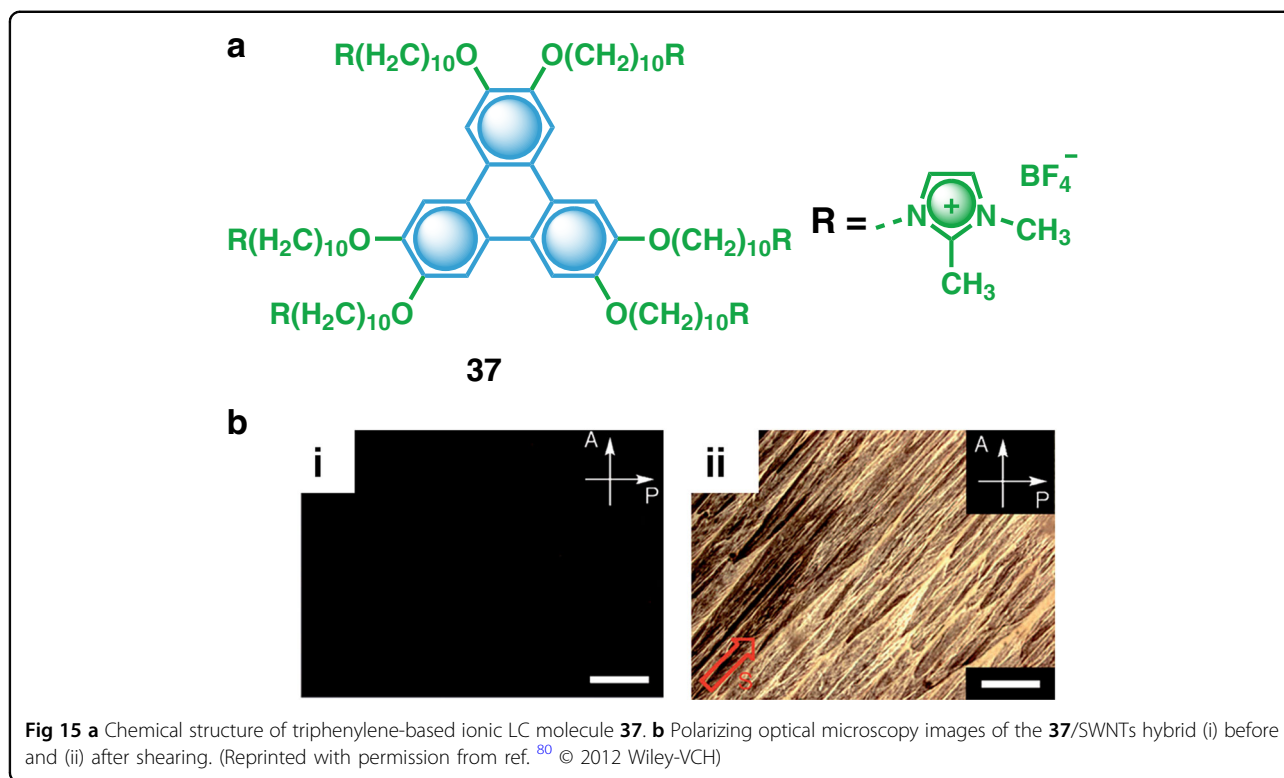


transferred to any substrate, and an additional layer of **21** could also be added to these conductive films by electropolymerization of 3-hexylthiophene. A regio-regular P3HT polymer, **45** (Fig. 17), was found to be suitable for dispersing SWNTs in organic solvents such as chloroform, THF and *o*-dichlorobenzene⁹¹. Interestingly, the hybrid **45**/SWNTs exhibited a nematic lyotropic LC phase, whereas the polymer **45** and the SWNTs alone did not show any lyotropic LC properties. The appearance of birefringence in the hybrid material was reported to depend upon the SWNT concentration. The nematic lyotropic LC phase of the hybrid could have resulted from the alignment of the individualized SWNTs at high concentrations.

Fluorene-based polymers such as poly(9,9-dialkylfluorene) (**46**) and poly(9,9-dialkylfluorene-*co*-3-alkylthiophene) (**47**, Fig. 17) have been reported to disperse SWNTs in organic solvents (up to 40%)⁸³. The dispersions

were stable for several weeks, even after the removal of the free polymer. The conductivities of the hybrid materials were comparable to that of pristine SWNTs but better than those of the polymers alone. In addition, the fluorene-based copolymer was used to separate chiral SWNTs through its selective diameter-dependent interaction with a mixture of SWNTs. By introducing π -conjugated molecules with a defined chiral phase, such as *R/S*-chiral binaphthyl groups, **48a, b** (Fig. 17), an enantiomeric pair of SWNTs could successfully be separated (Table 2)⁹².

A pyrene-tethered poly(phenylene acetylene) polymer, **49** (Fig. 17), was shown to disperse MWNTs in solvents such as CHCl_3 and THF⁹³. The higher solubility of the hybrid material was attributed to the π - π interaction of the MWNTs with the π -conjugated polymer as well as the extended π -surface of the pyrene moiety. The hybrid materials exhibited bi-polar behavior in photovoltaic



devices due to the uniform mixing of n-type MWNTs and p-type polymers in addition to photoinduced charge transfer between them (Table 2). All the details of the synthetic routes, properties and applications of carbon nanotube-based hybrid materials are summarized in Table 2.

Conclusions

The various reports discussed in this review reiterate the importance of functional hybrid materials consisting of π -conjugated organic small molecules/polymers and gelators with CNTs/graphene/graphene derivatives in a wide range of applications. A large number of π -conjugated systems have been exploited for the preparation of hybrid materials with intriguing optical and electronic properties. The insights gained from these studies over the years have helped researchers to design new materials with improved properties. For example, small aromatic molecules such as pyrene, perylene, naphthalene, and anthracene with appropriate functional groups have been designed and utilized in the preparation of self-assembled hybrid materials with CNTs and graphene/graphene derivatives. Moreover, the incorporation of these carbon nanomaterials in gel media improves the physical and mechanical properties of the hybrid systems relative to those of the individual counterparts. The extent of improvement in the material properties

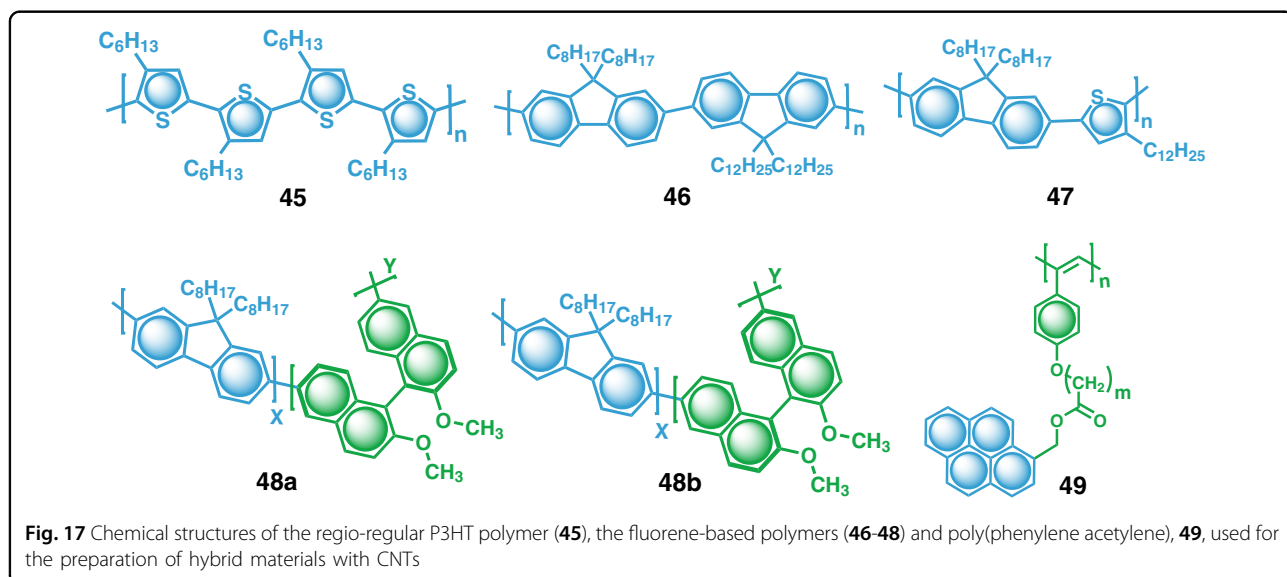
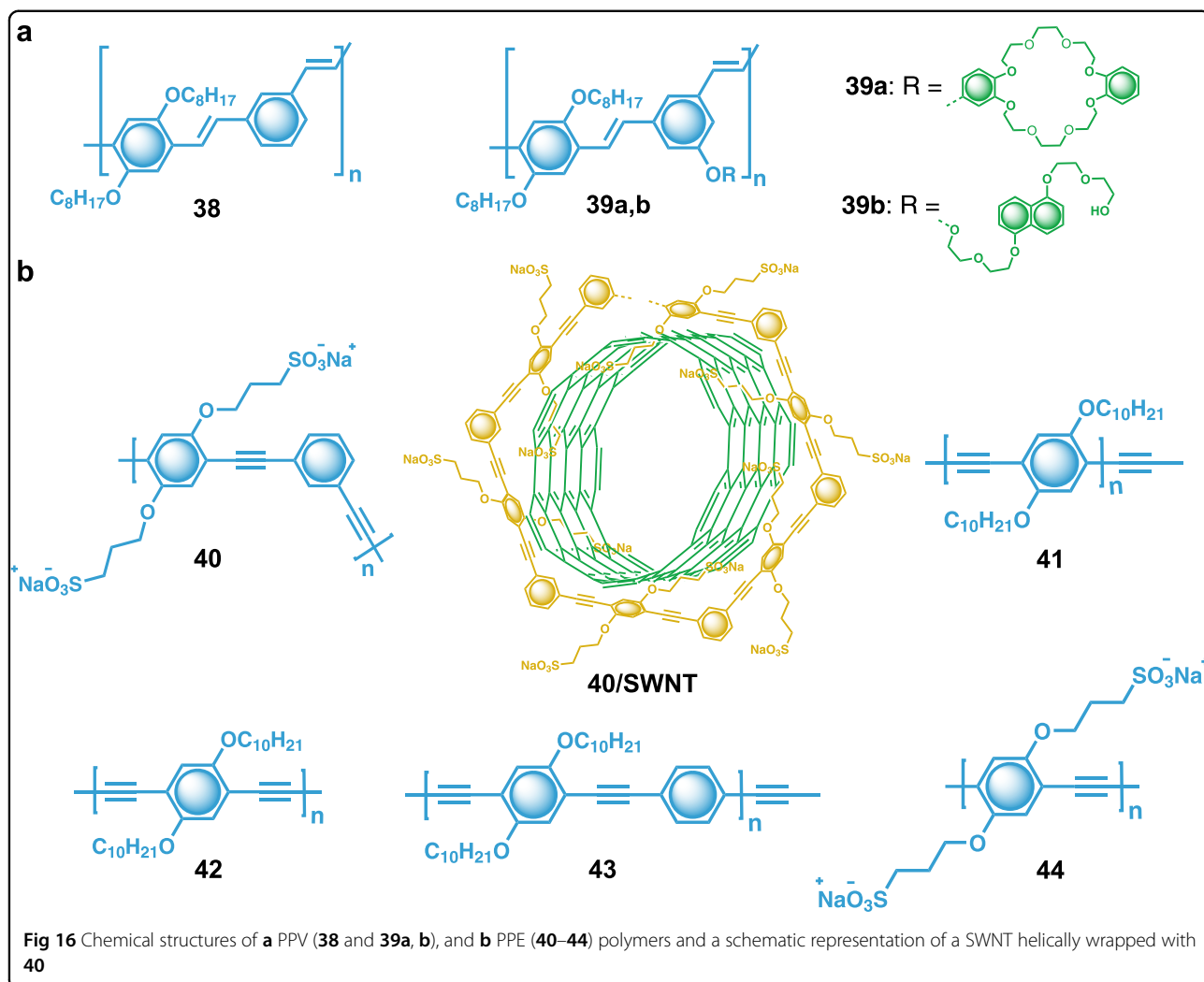
depends mainly on the strength of the noncovalent interactions between the carbon nanomaterials and the molecules that undergo self-assembly. The preparation of these hybrid materials via supramolecular self-assembly has several advantages, such as facilitating the solution processability of carbon nanomaterials while preserving their inherent electronic properties. Hybrid materials composed of conducting polymers such as polyaniline, polypyrrole, and polythiophene have potential for application in novel light-harvesting systems, solar cells, and organic field-effect transistors. Thus, the noncovalent functionalization of carbon allotropes with aromatic molecules/polymers and gelators is a promising strategy for realizing hybrid materials with potential applications. However, a breakthrough in the practical use of these hybrid materials is yet to come, and this unmet need will further drive research in this area.

Acknowledgements

A.A. thanks SERB, DST, Government of India for a J.C. Bose National Fellowship (SERB Order No. SB/S2/JCB-11/2014). B.V. and G.D. acknowledge CSIR, Government of India for research fellowships. V.K.P. thanks DST-SERB, Government of India for a Young Scientist Fellowship (SB/FT/CS-131/2014).

Author details

¹Photosciences and Photonics Section, Chemical Sciences and Technology Division, CSIR-National Institute for Interdisciplinary Science and Technology (CSIR-NIIST), Thiruvananthapuram 695019, India. ²Academy of Scientific and Innovative Research (AcSIR), CSIR-NIIST Campus, Thiruvananthapuram 695019, India



Conflict of interest

The authors declare that they have no conflict of interest.

Publisher's note

Springer Nature remains neutral with regard to jurisdictional claims in published maps and institutional affiliations.

Received: 31 July 2017 Revised: 1 November 2017 Accepted: 1 January 2018.

Published online: 9 April 2018

References

- Gómez-Romero, P. & Sanchez, C. *Functional hybrid materials* (Wiley-VCH Verlag GmbH & Co., Weinheim, Germany, 2005).
- Kickelbick, G. Hybrid materials—past, present and future. *Hybrid Mater.* **1**, 39–51 (2014).
- Sanchez, C., Arribart, H. & Giraud Guille, M. M. Biomimetic and bioinspiration as tools for the design of innovative materials and systems. *Nat. Mater.* **4**, 277–288 (2005).
- Wegst, U. G. K., Bai, H., Saiz, E., Tomsia, A. P. & Ritchie, R. O. Bioinspired structural materials. *Nat. Mater.* **14**, 23–36 (2015).
- Aida, T., Meijer, E. W. & Stupp, S. I. Functional supramolecular polymers. *Science* **335**, 813–817 (2012).
- Maggini, L. & Bonifazi, D. Hierarchical luminescent organic architectures: design, synthesis, self-assembly, self-organization and functions. *Chem. Soc. Rev.* **41**, 211–241 (2012).
- Moulin, E., Cid, J. J. & Giuseppone, N. Advances in supramolecular electronics - from randomly self-assembled nanostructures to addressable self-organized interconnects. *Adv. Mater.* **25**, 477–487 (2013).
- Yagai, S. Supramolecularly engineered functional π -assemblies based on complementary hydrogen-bonding interactions. *Bull. Chem. Soc. Jpn* **88**, 28–58 (2015).
- Jain, A. & George, S. J. New directions in supramolecular electronics. *Mater. Today* **18**, 206–214 (2015).
- Würthner, F. et al. Perylene bisimide dye assemblies as archetype functional supramolecular materials. *Chem. Rev.* **116**, 962–1052 (2016).
- Zhao, Y.-L. & Stoddart, J. F. Noncovalent functionalization of single-walled carbon nanotubes. *Acc. Chem. Res.* **42**, 1161–1171 (2009).
- Babu, S. S., Praveen, V. K. & Ajayaghosh, A. Functional π -gelators and their applications. *Chem. Rev.* **114**, 1973–2129 (2014).
- Srinivasan, S. & Ajayaghosh, A. *Interaction of carbon nanotubes and small molecules in Supramolecular soft matter: applications in materials and organic electronics* (ed. Nakanishi, T.) 381–406 (John Wiley & Sons, Inc., Hoboken, New Jersey, USA, 2011).
- Bhattacharya, S. & Samanta, S. K. Soft-nanocomposites of nanoparticles and nanocarbons with supramolecular and polymer gels and their applications. *Chem. Rev.* **116**, 11967–12028 (2016).
- Ghosh, S., Praveen, V. K. & Ajayaghosh, A. The chemistry and applications of π -gels. *Annu. Rev. Mater. Res.* **46**, 235–262 (2016).
- Fukushima, T. & Aida, T. Ionic liquids for soft functional materials with carbon nanotubes. *Chem. — Eur. J.* **13**, 5048–5058 (2007).
- Aono, M. & Ariga, K. The way to nanoarchitectonics and the way of nanoarchitectonics. *Adv. Mater.* **28**, 989–992 (2016).
- Ariga, K., Ji, Q., Nakanishi, W., Hill, J. P. & Aono, M. Nanoarchitectonics: a new materials horizon for nanotechnology. *Mater. Horiz.* **2**, 406–413 (2015).
- Umadevi, D., Panigrahi, S. & Sastry, G. Noncovalent interaction of carbon nanostructures. *Acc. Chem. Res.* **47**, 2574–2581 (2014).
- Geim, A. K. Graphene: status and prospects. *Science* **324**, 1530–1534 (2009).
- Rao, C. N. R., Sood, A. K., Subrahmanyam, K. S. & Govindaraj, A. Graphene: the new two-dimensional nanomaterial. *Angew. Chem. Int. Ed.* **48**, 7752–7777 (2009).
- Weiss, N. O. et al. Graphene: an emerging electronic material. *Adv. Mater.* **24**, 5782–5825 (2012).
- Jarivwala, D., Sangwan, V. K., Lauhon, L. J., Marks, T. J. & Hersam, M. C. Carbon nanomaterials for electronics, optoelectronics, photovoltaics, and sensing. *Chem. Soc. Rev.* **42**, 2824–2860 (2013).
- Li, C. & Shi, G. Functional gels based on chemically modified graphenes. *Adv. Mater.* **26**, 3992–4012 (2014).
- Bai, H., Li, C. & Shi, G. Functional composite materials based on chemically converted graphene. *Adv. Mater.* **23**, 1089–1115 (2011).
- Ariga, K., Ji, Q., Hill, J. P., Bando, Y. & Aono, M. Forming nanomaterials as layered functional structures toward materials nanoarchitectonics. *NPG Asia Mater.* **4**, e17 (2012).
- Adhikari, B., Nanda, J. & Banerjee, A. Pyrene-containing peptide-based fluorescent organogels: inclusion of graphene into the organogel. *Chem. Eur. J.* **17**, 11488–11496 (2011).
- Nanda, J., Biswas, A., Adhikari, B. & Banerjee, A. A gel-based trihybrid system containing nanofibers, nanosheets, and nanoparticles: modulation of the rheological property and catalysis. *Angew. Chem. Int. Ed.* **52**, 5041–5045 (2013).
- Srinivasan, S. et al. Ordered supramolecular gels based on graphene oxide and tetracationic cyclophanes. *Adv. Mater.* **26**, 2725–2729 (2014).
- Bai, H., Sheng, K., Zhang, P., Li, C. & Shi, G. Graphene oxide/conducting polymer composite hydrogels. *J. Mater. Chem.* **21**, 18653–18658 (2011).
- Srinivasan, S., Shin, W. H., Choi, J. W. & Coskun, A. A bifunctional approach for the preparation of graphene and ionic liquid-based hybrid gels. *J. Mater. Chem. A* **1**, 43–48 (2013).
- Vedhanarayanan, B., Babu, B., Shajumon, M. M. & Ajayaghosh, A. Exfoliation of reduced graphene oxide with self-assembled π -gelators for improved electrochemical performance. *ACS Appl. Mater. Interfaces* **9**, 19417–19426 (2017).
- Harada, A., Takashima, Y. & Yamaguchi, H. Cyclodextrin-based supramolecular polymers. *Chem. Soc. Rev.* **38**, 875–882 (2009).
- Liu, J., Chen, G. & Jiang, M. Supramolecular hybrid hydrogels from non-covalently functionalized graphene with block copolymers. *Macromolecules* **44**, 7682–7691 (2011).
- Zhu, C.-H., Lu, Y., Peng, J., Chen, J.-F. & Yu, S.-H. Photothermally sensitive poly(*n*-isopropylacrylamide)/graphene oxide nanocomposite hydrogels as remote light-controlled liquid microvalves. *Adv. Funct. Mater.* **22**, 4017–4022 (2012).
- An, X. et al. Stable aqueous dispersions of noncovalently functionalized graphene from graphite and their multifunctional high-performance applications. *Nano Lett.* **10**, 4295–4301 (2010).
- Jang, J.-H., Rangappa, D., Kwon, Y.-U. & Honma, I. Direct preparation of 1-PSA modified graphene nanosheets by supercritical fluidic exfoliation and its electrochemical properties. *J. Mater. Chem.* **21**, 3462–3466 (2011).
- Lee, D.-W., Kim, T. & Lee, M. An amphiphilic pyrene sheet for selective functionalization of graphene. *Chem. Commun.* **47**, 8259–8261 (2011).
- Khanra, P. et al. Electrochemical performance of reduced graphene oxide surface-modified with 9-anthracene carboxylic acid. *RSC Adv.* **5**, 6443–6451 (2015).
- Ghosh, A., Rao, K. V., George, S. J. & Rao, C. N. R. Noncovalent functionalization, exfoliation, and solubilization of graphene in water by employing a fluorescent coronene carboxylate. *Chem. Eur. J.* **16**, 2700–2704 (2010).
- Su, Q. et al. Composites of graphene with large aromatic molecules. *Adv. Mater.* **21**, 3191–3195 (2009).
- Xu, Y. et al. Chemically converted graphene induced molecular flattening of 5,10,15,20-tetrakis(1-methyl-4-pyridinio)porphyrin and its application for optical detection of cadmium(II) ions. *J. Am. Chem. Soc.* **131**, 13490–13497 (2009).
- Geng, J. & Jung, H.-T. Porphyrin functionalized graphene sheets in aqueous suspensions: From the preparation of graphene sheets to highly conductive graphene films. *J. Phys. Chem. C* **114**, 8227–8234 (2010).
- Jiang, B.-P. et al. Graphene loading water-soluble phthalocyanine for dual-modality photothermal/photodynamic therapy via a one-step method. *J. Mater. Chem. B* **2**, 7141–7148 (2014).
- Wang, Y., Kurunthu, D., Scott, G. W. & Bardeen, C. J. Fluorescence quenching in conjugated polymers blended with reduced graphitic oxide. *J. Phys. Chem. C* **114**, 4153–4159 (2010).
- Yang, H. et al. Stable, conductive supramolecular composite of graphene sheets with conjugated polyelectrolyte. *Langmuir* **26**, 6708–6712 (2010).
- Wang, H., Hao, Q., Yang, X., Lu, L. & Wang, X. Effect of graphene oxide on the properties of its composite with polyaniline. *ACS Appl. Mater. Interfaces* **2**, 821–828 (2010).
- Zhang, K., Zhang, L. L., Zhao, X. S. & Wu, J. Graphene/polyaniline nanofiber composites as supercapacitor electrodes. *Chem. Mater.* **22**, 1392–1401 (2010).
- Bai, H., Xu, Y., Zhao, L., Li, C. & Shi, G. Noncovalent functionalization of graphene sheets by sulfonated polyaniline. *Chem. Commun.* 1667–1669 (2009).

50. Gu, Z. et al. Synthesis and characterization of polypyrrole/graphite oxide composite by in situ emulsion polymerization. *J. Polym. Sci. B Polym. Phys.* **48**, 1329–1335 (2010).
51. Chunder, A., Liu, J. & Zhai, L. Reduced graphene oxide/poly(3-hexylthiophene) supramolecular composites. *Macromol. Rapid Commun.* **31**, 380–384 (2010).
52. Liu, Q. et al. Polymer photovoltaic cells based on solution-processable graphene and P3HT. *Adv. Funct. Mater.* **19**, 894–904 (2009).
53. Xu, Y. et al. A hybrid material of graphene and poly(3,4-ethyldioxythiophene) with high conductivity, flexibility, and transparency. *Nano Res.* **2**, 343–348 (2009).
54. Choi, K. S., Liu, F., Choi, J. S. & Seo, T. S. Fabrication of free-standing multilayered graphene and poly(3,4-ethylenedioxythiophene) composite films with enhanced conductive and mechanical properties. *Langmuir* **26**, 12902–12908 (2010).
55. Srinivasan, S., Babu, S. S., Praveen, V. K. & Ajayaghosh, A. Carbon nanotube triggered self-assembly of oligo(*p*-phenylene vinylene)s to stable hybrid π -gels. *Angew. Chem. Int. Ed.* **47**, 5746–5749 (2008).
56. López-Andarias, J. et al. Controlling the crystalline three-dimensional order in bulk materials by single-wall carbon nanotubes. *Nat. Commun.* **5**, 3763 (2014).
57. Tian, Y. et al. Fabrication of organogels composed from carbon nanotubes through a supramolecular approach. *New J. Chem.* **34**, 2847–2852 (2010).
58. Samanta, S. K., Pal, A., Bhattacharya, S. & Rao, C. N. R. Carbon nanotube reinforced supramolecular gels with electrically conducting, viscoelastic and near-infrared sensitive properties. *J. Mater. Chem.* **20**, 6881–6890 (2010).
59. Mandal, D., Kar, T. & Das, P. K. Pyrene-based fluorescent ambidextrous gelators: scaffolds for mechanically robust SWNT–gel nanocomposites. *Chem. Eur. J.* **20**, 1349–1358 (2014).
60. Roy, S. & Banerjee, A. Functionalized single walled carbon nanotube containing amino acid based hydrogel: a hybrid nanomaterial. *RSC Adv.* **2**, 2105–2111 (2012).
61. Roy, S., Baral, A. & Banerjee, A. An amino-acid-based self-healing hydrogel: modulation of the self-healing properties by incorporating carbon-based nanomaterials. *Chem. Eur. J.* **19**, 14950–14957 (2013).
62. Star, A. & Stoddart, F. J. Dispersion and solubilization of single-walled carbon nanotubes with a hyperbranched polymer. *Macromolecules* **35**, 7516–7520 (2002).
63. Liang, S., Chen, G., Peddle, J. & Zhao, Y. Reversible dispersion and releasing of single-walled carbon nanotubes by a stimuli-responsive TTFV-phenylacetylene polymer. *Chem. Commun.* **48**, 3100–3102 (2012).
64. Vedhanarayanan, B., Nair, V. S., Nair, V. C. & Ajayaghosh, A. Formation of coaxial nanocables with amplified supramolecular chirality through an interaction between carbon nanotubes and a chiral π -gelator. *Angew. Chem. Int. Ed.* **55**, 10345–10349 (2016).
65. Ogoshi, T., Takashima, Y., Yamaguchi, H. & Harada, A. Chemically-responsive sol–gel transition of supramolecular single-walled carbon nanotubes (SWNTs) hydrogel made by hybrids of SWNTs and cyclodextrins. *J. Am. Chem. Soc.* **129**, 4878–4879 (2007).
66. Tamesue, S., Takashima, Y., Yamaguchi, H., Shinkai, S. & Harada, A. Photochemically controlled supramolecular curdlan/single-walled carbon nanotube composite gel: preparation of molecular distaff by cyclodextrin modified curdlan and phase transition control. *Eur. J. Org. Chem.* **2011**, 2801–2806 (2011).
67. Malicka, J. M. et al. Ultrasound stimulated nucleation and growth of a dye assembly into extended gel nanostructures. *Chem. Eur. J.* **19**, 12991–13001 (2013).
68. Guldi, D. M. et al. Functional single-wall carbon nanotube nanohybrids-associating SWNTs with water-soluble enzyme model systems. *J. Am. Chem. Soc.* **127**, 9830–9838 (2005).
69. Guldi, D. M. et al. Single-wall carbon nanotubes as integrative building blocks for solar-energy conversion. *Angew. Chem., Int. Ed.* **44**, 2015–2018 (2005).
70. Guldi, D. M., Rahman, G. M. A., Zerbetto, F. & Prato, M. Carbon nanotubes in electron donor-acceptor nanocomposites. *Acc. Chem. Res.* **38**, 871–878 (2005).
71. Paloniemi, H. et al. Water-soluble full-length single-wall carbon nanotube polyelectrolytes: preparation and characterization. *J. Phys. Chem. B* **109**, 8634–8642 (2005).
72. Yu, M. et al. Spatially controllable DNA condensation by a water-soluble supramolecular hybrid of single-walled carbon nanotubes and β -cyclodextrin-tethered ruthenium complexes. *Chem. Eur. J.* **16**, 1168–1174 (2010).
73. Backes, C., Schmidt, C. D., Hauke, F., Böttcher, C. & Hirsch, A. High population of individualized SWCNTs through the adsorption of water-soluble perylenes. *J. Am. Chem. Soc.* **131**, 2172–2184 (2009).
74. Backes, C. et al. Nanotube surfactant design: the versatility of water-soluble perylene bisimides. *Adv. Mater.* **22**, 788–802 (2010).
75. Backes, C., Schmidt, C. D., Hauke, F. & Hirsch, A. Perylene-based nanotweezers: enrichment of larger-diameter single-walled carbon nanotubes. *Chem. Asian J.* **6**, 438–444 (2011).
76. Tsarfaty, Y. et al. Dispersing perylene diimide/SWCNT hybrids: structural insights at the molecular level and fabricating advanced materials. *J. Am. Chem. Soc.* **137**, 7429–7440 (2015).
77. Srinivasan, S., Praveen, V. K., Philip, R. & Ajayaghosh, A. Bioinspired superhydrophobic coatings of carbon nanotubes and linear π systems based on the “bottom-up” self-assembly approach. *Angew. Chem. Int. Ed.* **47**, 5750–5754 (2008).
78. Llanes-Pallas, A. et al. Modular engineering of H-bonded supramolecular polymers for reversible functionalization of carbon nanotubes. *J. Am. Chem. Soc.* **133**, 15412–15424 (2011).
79. Maggini, L. et al. Azobenzene-based supramolecular polymers for processing MWCNTs. *Nanoscale* **5**, 634–645 (2013).
80. Lee, J. J. et al. Discotic ionic liquid crystals of triphenylene as dispersants for orienting single-walled carbon nanotubes. *Angew. Chem. Int. Ed.* **51**, 8490–8494 (2012).
81. Samanta, S. K. et al. Conjugated polymer-assisted dispersion of single-wall carbon nanotubes: the power of polymer wrapping. *Acc. Chem. Res.* **47**, 2446–2456 (2014).
82. Chen, Y. et al. Highly selective dispersion of carbon nanotubes by using poly(phenyleneethynylene)-guided supermolecular assembly. *Small* **9**, 870–875 (2013).
83. Cheng, F., Imin, P., Maunders, C., Botton, G. & Adronov, A. Soluble, discrete supramolecular complexes of single-walled carbon nanotubes with fluorene-based conjugated polymers. *Macromolecules* **41**, 2304–2308 (2008).
84. Lei, T., Chen, X., Pitner, G., Wong, H. S. & Bao, Z. Removable and recyclable conjugated polymers for highly selective and high-yield dispersion and release of low-cost carbon nanotubes. *J. Am. Chem. Soc.* **138**, 802–805 (2016).
85. Steuerman, D. W. et al. Interactions between conjugated polymers and single-walled carbon nanotubes. *J. Phys. Chem. B* **106**, 3124–3130 (2002).
86. Star, A. et al. Noncovalent side-wall functionalization of single-walled carbon nanotubes. *Macromolecules* **36**, 553–560 (2003).
87. Chen, Y. et al. Highly selective dispersion of carbon nanotubes by using poly(phenyleneethynylene)-guided supermolecular assembly. *Small* **9**, 870–875 (2013).
88. Rice, N. A., Soper, K., Zhou, N., Merschrod, E. & Zhao, Y. Dispersing as-prepared single-walled carbon nanotube powders with linear conjugated polymers. *Chem. Commun.* **0**, 4937–4939 (2006).
89. Kang, Y. K. et al. Helical wrapping of single-walled carbon nanotubes by water soluble poly(*p*-phenyleneethynylene). *Nano Lett.* **9**, 1414–1418 (2009).
90. Gu, H. & Swager, T. M. Fabrication of free-standing, conductive, and transparent carbon nanotube films. *Adv. Mater.* **20**, 4433–4437 (2008).
91. Lee, H. et al. Lyotropic liquid-crystalline solutions of high-concentration dispersions of single-walled carbon nanotubes with conjugated polymers. *Small* **5**, 1019–1024 (2009).
92. Akazaki, K., Toshimitsu, F., Ozawa, H., Fujigaya, T. & Nakashima, N. Recognition and one-pot extraction of right- and left-handed semiconducting single-walled carbon nanotube enantiomers using fluorene-bisphthalol chiral copolymers. *J. Am. Chem. Soc.* **134**, 12700–12707 (2012).
93. Yuan, W. et al. Wrapping carbon nanotubes in pyrene-containing poly(phenylacetylene) chains: solubility, stability, light emission, and surface photovoltaic properties. *Macromolecules* **39**, 8011–8020 (2006).